Symmetries of meson correlators in high-temperature QCD with physical $(u/d,s,c)$ domain-wall quarks

Ting-Wai Chiu[*]

Department of Physics, National Taiwan Normal University, Taipei, Taiwan 11677, Republic of China;
Institute of Physics, Academia Sinica, Taipei, Taiwan 11529, Republic of China;
Physics Division, National Center for Theoretical Sciences, Taipei, Taiwan 10617, Republic of China
and Center for Theoretical Physics, Department of Physics, National Taiwan University,
Taipei, Taiwan 10617, Republic of China

The correlation functions of meson interpolators in $N_f = 2 + 1 + 1$ lattice QCD with optimal domain-wall quarks at the physical point are studied for six temperatures in the range $T \sim 190$–770 MeV. The meson interpolators include a complete set of Dirac bilinears, and each for six combinations of quark flavors. In this paper, we focus on the meson correlators of u and d quarks, and we discuss their implications for the effective restoration of $U(1)_A$ and $SU(2)_L \times SU(2)_R$ chiral symmetries, as well as the emergence of approximate $SU(2)_{\text{CS}}$ chiral spin symmetry.

I. INTRODUCTION

It is important to understand the nature of strongly interacting matter at high temperatures, which is crucial for the mechanism of matter creation in the early Universe, as well as in relativisitic heavy ion collision experiments such as those at the RHIC and LHC. A first step toward this goal is to find out the symmetries of QCD at high temperatures, since the nature of matter is likely to be unveiled from its symmetries.

At low temperatures $T < T_c$, quarks and gluons are confined in hadrons, and the chiral symmetry of QCD is spontaneously broken, with the nonzero chiral condensate $[\Sigma(T) \neq 0]$:

$$\Sigma(T) = -\lim_{m_q \to 0} \lim_{V \to \infty} \frac{T}{V} \int_0^{1/T} dt \int_V d^3x \langle \text{Tr}(D_c + m_q)^{-1} \rangle. \quad (1)$$

Moreover, the $U(1)_A$ symmetry is explicitly broken by the chiral anomaly due to the quantum fluctuations of topologically nontrivial gauge fields.

Since the quark mass explicitly breaks the $U(1)_A$ symmetry and the chiral symmetry, determining whether the $U(1)_A$ symmetry and the chiral symmetry are broken/restored at any T should be performed in the massless limit. Nevertheless, for QCD with physical (u, d, s, c, b) quarks with nonzero quark masses, as the temperature T is increased, the $SU(n_f)_L \times SU(n_f)_R$ chiral symmetry is effectively restored successively from $n_f = 2$ to 3, 4, and 5—say, as $T \nearrow T_c^{u/d} \nearrow T_c^s \nearrow T_c^c \nearrow T_c^b$. Since the $SU(2)_L \times SU(2)_R$ chiral symmetry of physical u and d quarks is effectively restored at $T \geq T_c^{u/d}$, its counterpart T_c^0 in QCD with massless (u, d, s, c, b) quarks is supposed to be at a lower temperature—i.e., $T_c^0 < T_c^{u/d}$. Now, assuming that the $U(1)_A$ symmetry in QCD with massless (u, d, s, c, b) quarks is also effectively restored at T_c^0, it is unclear whether the $U(1)_A$ symmetry of u and d quarks in QCD with physical (u, d, s, c, b) quarks is also effectively restored at $T \geq T_c^{u/d}$, or at higher temperatures $T \geq T_1^{u/d} \gtrsim T_c^{u/d}$.

Since 1987 [1], there have been many lattice studies using spatial meson correlators (and their screening masses) to investigate the effective restoration of $U(1)_A$ and $SU(2)_L \times SU(2)_R$ chiral symmetries in high-temperature QCD—see, e.g., Ref. [2] and references therein. In this paper, we will use the degeneracies of meson correlators of u and d quarks to determine the effective restoration or the emergence of any exact/approximate symmetries in high-temperature QCD, as discussed in Sec. II. For example, we use the degeneracy of meson correlators of vectors ($V_k \equiv \bar{u}\gamma_k d$) and axial vectors ($A_k \equiv \bar{u}\gamma_5\gamma_k d$) to determine the effective restoration of the $SU(2)_L \times SU(2)_R$ chiral symmetry of u and d quarks, and the degeneracy of the meson correlators of the scalar ($S \equiv \bar{u}d$) and the pseudoscalar ($P \equiv \bar{u}\gamma_5 d$) to determine the effective restoration of the $U(1)_A$ symmetry of u and d quarks.

[*]twchiu@phys.ntu.edu.tw

Now, the question is whether $U(1)_A$ and $SU(2)_L \times SU(2)_R$ are the only symmetries of QCD with physical (u, d, s, c, b) quarks for $T \geq T_1^{u/d} \gtrsim T_c^{u/d}$, all the way up to the temperatures where the effective coupling among quarks and gluons becomes sufficiently weak (screened), and the quarks and gluons behave like deconfined particles forming the quark-gluon plasma. In particular, it is interesting to find out whether there are any emergent symmetries which are manifested in observables (e.g., hadron correlators) but not in the QCD action. Moreover, one may ask whether quarks are deconfined or confined inside these hadron-like objects for temperatures $T \gtrsim T_c^{u/d}$. In the latter case, the properties of these hadron-like objects would be quite different from those at $T < T_c^{u/d}$, since the chiral symmetry has been restored with $\Sigma = 0$.

Recently, it has been observed that in $N_f = 2$ lattice QCD with domain-wall fermions, at temperatures $T \sim 220$–500 MeV $\sim (1.2$–$2.8)T_c$ (where $T_c \sim 175$ MeV for $N_f = 2$ lattice QCD), a larger symmetry group $SU(2)_{CS}$ [with $U(1)_A$ as a subgroup] [3,4] is approximately manifested in the multiplets of correlators of the $J = 1$ meson interpolators [5,6], as an approximate emergent symmetry in high-temperature QCD. This suggests the possible existence of hadron-like objects which are predominantly bound by chromoelectric interactions into color singlets for a range of temperatures above T_c. Now, the question is one of identifying the scenario of the emergence of approximate $SU(2)_{CS}$ chiral spin symmetry in QCD with dynamical light and heavy quarks. This motivates the present study.

In this paper, we study the temporal and spatial correlation functions of meson interpolators in $N_f = 2 + 1 + 1$ lattice QCD with (u, d, s, c) optimal domain-wall quarks at the physical point on the $32^3 \times (16, 12, 10, 8, 6, 4)$ lattices for temperatures in the range $T \sim 190$–770 MeV. The meson interpolators include a complete set of Dirac bilinears (scalar, pseudoscalar, vector, axial vector, tensor vector, and axial-tensor vector), and each for six combinations of quark flavors ($\bar{u}d$, $\bar{u}s$, $\bar{u}c$, $\bar{s}c$, $\bar{s}s$, and $\bar{c}c$). We discuss the implications of these results for the effective restoration of the $SU(2)_L \times SU(2)_R$ and $U(1)_A$ chiral symmetries, as well as the emergence of approximate $SU(2)_{CS}$ chiral spin symmetry. In this paper, we focus on the meson correlators of u and d quarks. The results of meson correlators with other flavor combinations ($\bar{u}s$, $\bar{u}c$, $\bar{s}c$, $\bar{s}s$, and $\bar{c}c$) will be analyzed in a forthcoming paper [7].

The outline of this paper is as follows: In Sec. II, we discuss the relationship between various symmetries [$SU(2)_L \times SU(2)_R$, $U(1)_A$, $SU(2)_{CS}$, and $SU(4)$] and the degeneracies of meson correlators. In Sec. III, the symmetry-breaking parameters for measuring various symmetries with the degeneracies of meson correlators are defined. In Sec. IV, the features of the gauge ensembles of $N_f = 2 + 1 + 1$ lattice QCD at the physical point for this study are outlined. The results of the temporal t correlators

for three temperatures in the range $T \simeq 190$–310 MeV are presented in Sec. V, while those of the spatial z correlators for six temperatures in the range $T \simeq 190$–770 MeV are presented in Sec. VI. We discuss their implications for the effective restoration of $SU(2)_L \times SU(2)_R$ and $U(1)_A$ chiral symmetries, and the emergence of the approximate $SU(2)_{CS}$ chiral spin symmetry. We also compare our results with those in $N_f = 2$ lattice QCD [5,6], as well as the noninteracting theory with free quarks. In Sec. VII, we conclude with some remarks.

II. SYMMETRIES AND MESON CORRELATORS

In this section, we discuss the relationship between the symmetry and the degeneracy of the meson correlators in high-temperature QCD.

The correlation function of the meson interpolator $\bar{q}_1 \Gamma q_2$ is measured according to the formula

$$C_\Gamma(t, \vec{x}) = \langle (\bar{q}_1 \Gamma q_2)_x (\bar{q}_1 \Gamma q_2)_0^\dagger \rangle$$
$$= \langle \text{tr}[\Gamma (D_c + m_1)_{0,x}^{-1} \Gamma (D_c + m_2)_{x,0}^{-1}] \rangle_{\text{confs}}, \quad (2)$$

where $(D_c + m_q)^{-1}$ denotes the valence quark propagator with quark mass m_q in lattice QCD with exact chiral symmetry, "tr" denotes the trace over the color and Dirac indices, and the brackets $\langle \cdots \rangle_{\text{confs}}$ denote averaging over the gauge configurations. Here, the label of a lattice site x is understood to stand for $(x_1, x_2, x_3, x_4) = (x, y, z, t)$, and the overall $\pm$ sign due to $\gamma_4 \Gamma^\dagger \gamma_4 = \pm \Gamma$ has been suppressed.

On a lattice of $N_x^3 \times N_t$ sites, the discrete Fourier transform of Eq. (2) gives

$$\tilde{C}_\Gamma(t, \vec{p}, T) = \sum_{x_1, x_2, x_3} \exp(i\vec{p} \cdot \vec{x}) C_\Gamma(t, \vec{x}), \quad T = \frac{1}{N_t a}, \quad (3)$$

which is related to the spectral function $\rho_\Gamma(\omega, \vec{p}, T)$ through the integral transform,

$$\tilde{C}_\Gamma(t, \vec{p}, T) = \int_0^\infty \frac{d\omega}{2\pi} \frac{\cosh[\omega(t - \frac{1}{2T})]}{\sinh(\frac{\omega}{2T})} \rho_\Gamma(\omega, \vec{p}, T). \quad (4)$$

The time-correlation function (t correlator) of the meson interpolator $\bar{q}_1 \Gamma q_2$ is defined as

$$C_\Gamma(t, T) = \sum_{x_1, x_2, x_3} C_\Gamma(t, \vec{x}), \quad (5)$$

which is equal to $\tilde{C}_\Gamma(t, \vec{p} = 0, T)$ and is related to the spectral function at $\vec{p} = 0$.

Alternatively, one can study the spatial correlation function in the z direction (z correlator):

$$C_\Gamma(z, T) = \sum_{x_1, x_2, x_4} C_\Gamma(t, \vec{x}), \quad T = \frac{1}{N_t a}, \quad (6)$$

which is related to the spectral function at $p_1 = p_2 = 0$ through the integral transform

$$C_\Gamma(z, T) = \int_0^\infty \frac{d\omega}{\pi\omega} \int_{-\infty}^{+\infty} \frac{dp_3}{2\pi} \exp(ip_3 z)\rho_\Gamma(\omega, p_3, T). \quad (7)$$

If any symmetry manifests in the z correlator, it should also appear in the spectral function $\rho(\omega, \vec{p}, T)$, since in thermal equilibrium, $\rho(\omega, \vec{p}, T) = \rho(\omega, |p|, T)$, which is isotropic in all directions of $\vec{p}$.

In the following, it is understood that $C_\Gamma(t, T)$ is normalized by $C_\Gamma(n_t = 1, T)$, and similarly $C_\Gamma(z, T)$ is normalized by $C_\Gamma(n_z = 1, T)$.

A. Classification of meson interpolators

The meson interpolators are classified according to their transformation properties as listed in Table I. The Γ matricies are given for the t correlators in the second column, and for the z correlators in the third column. Note that V_4 and A_4 are omitted for the t correlators, since $C_{V_4}(t)$ and $C_{A_4}(t)$ do not propagate in the t direction when the chiral symmetry of u and d quarks is effectively restored for $T > T_c$. Similarly, V_3 and A_3 are omitted for the z correlators.

For the vector meson correlators, the rotational symmetry in the continuum is reduced to the discrete permutation symmetry on the lattice. For the t correlators, the rotational symmetry becomes the S_3 symmetry of the x, y, and z components, which gives $C_{V_1} = C_{V_2} = C_{V_3}$, $C_{A_1} = C_{A_2} = C_{A_3}$, $C_{T_1} = C_{T_2} = C_{T_3}$, and $C_{X_1} = C_{X_2} = C_{X_3}$. For the z correlators, it becomes the S_2 symmetry of the x and y components, which gives $C_{V_1} = C_{V_2}$, $C_{A_1} = C_{A_2}$, $C_{T_1} = C_{T_2}$, and $C_{X_1} = C_{X_2}$.

B. $U(1)_A$ symmetry

For the scalar (S) and the pseudoscalar (P) bilinears, their correlators can be transformed into each other by the global $U(1)_A$ transformations

$$q(x) \to \exp(i\gamma_5\theta)q(x), \quad \bar{q}(x) \to \bar{q}(x)\gamma_4 \exp(-i\gamma_5\theta)\gamma_4. \quad (8)$$

TABLE I. The classification of meson interpolators $\bar{q}_1\Gamma q_2$, and their names and notations. The Γ matricies in the second column are for the t correlators, while those in the third column are for the z correlators.

Name and notation	Γ (for t correlators)	Γ (for z correlators)
Scalar (S)	$\mathbb{1}$	$\mathbb{1}$
Pseudocalar (P)	γ_5	γ_5
Vector (V_k)	γ_k ($k = 1, 2, 3$)	γ_k ($k = 1, 2, 4$)
Axial vector (A_k)	$\gamma_5\gamma_k$ ($k = 1, 2, 3$)	$\gamma_5\gamma_k$ ($k = 1, 2, 4$)
Tensor vector (T_k)	$\gamma_4\gamma_k$ ($k = 1, 2, 3$)	$\gamma_3\gamma_k$ ($k = 1, 2, 4$)
Axial-tensor vector (X_k)	$\gamma_5\gamma_4\gamma_k$ ($k = 1, 2, 3$)	$\gamma_5\gamma_3\gamma_k$ ($k = 1, 2, 4$)

Similarly, for the tensor vector (T_k) and the axial-tensor vector (X_k), their correlators can be transformed into each other by the global $U(1)_A$ transformations. If $U(1)_A$ is effectively restored for $T \gtrsim T_1^q$ (where T_1^q depends on the masses of q_1 and q_2), the correlators of the scalar (S) and pseudoscalar (P) are degenerate, and also those of tensor vectors (T_k) and axial-tensor vectors (X_k)—i.e.,

$$C_S(t) = C_P(t); \quad C_{T_k}(t) = C_{X_k}(t), \quad k = 1, 2, 3,$$
$$C_S(z) = C_P(z); \quad C_{T_k}(z) = C_{X_k}(z), \quad k = 1, 2, 4.$$

Thus, the effective restoration of the $U(1)_A$ symmetry is equivalent to the emergence of two multiplets

$$(S, P); (\{T_k\}, \{X_k\}), \quad (9)$$

where $k = 1, 2, 3$ for t correlators and $k = 1, 2, 4$ for z correlators.

C. $SU(2)_L \times SU(2)_R$ flavor chiral symmetry

For the $SU(2)$ flavor doublet $q = (q_1, q_2)^T$, we consider the vector bilinears (V_k)

$$\bar{q}(x)\gamma_k \frac{\tau_\pm}{2} q(x), \quad \tau_\pm = \tau_1 \pm i\tau_2,$$

where $\{\tau_1, \tau_2, \tau_3\}$ are Pauli matrices, and $\{\tau_i/2, i = 1, 2, 3\}$ are the generators of the $SU(2)$ group in the flavor space. Similarly, the axial-vector bilinears (A_k) can be written as

$$\bar{q}(x)\gamma_5\gamma_k \frac{\tau_\pm}{2} q(x).$$

The correlators of vector and axial-vector bilinears can be transformed into each other by the flavor nonsinglet axial rotations

$$q(x) \to \exp\left(i\gamma_5 \frac{\vec{\tau}}{2} \cdot \vec{\theta}\right)q(x),$$
$$\bar{q}(x) \to \bar{q}(x)\gamma_4 \exp\left(-i\gamma_5 \frac{\vec{\tau}}{2} \cdot \vec{\theta}\right)\gamma_4. \quad (10)$$

If the $SU(2)_L \times SU(2)_R$ chiral symmetry of the flavor doublet is effectively restored for $T \gtrsim T_c^q$ (where T_c^q depends on the masses of q_1 and q_2), the correlators of the vector bilinears (V_k) and the axial-vector bilinears (A_k) are degenerate—i.e., $C_{V_k} = C_{A_k}$. Thus, the effective restoration of $SU(2)_L \times SU(2)_R$ chiral symmetry is equivalent to the emergence of the multiplet

$$(\{V_k\}, \{A_k\}), \quad (11)$$

where $k = 1, 2, 3$ for t correlators and $k = 1, 2, 4$ for z correlators.

D. $SU(2)_{CS}$ chiral spin symmetry

The $SU(2)_{CS}$ chiral spin transformations [3,4] are defined by

$$q(x) \rightarrow \exp\left(i\frac{\vec{\Sigma}_\mu}{2} \cdot \vec{\theta}\right) q(x),$$

$$\bar{q}(x) \rightarrow \bar{q}(x)\gamma_4 \exp\left(-i\frac{\vec{\Sigma}_\mu}{2} \cdot \vec{\theta}\right)\gamma_4, \quad \mu = 1, 2, 3, 4, \quad (12)$$

where $\vec{\Sigma}_\mu = \{\gamma_\mu, i\gamma_\mu\gamma_5, \gamma_5\}$, and $\vec{\theta}$ are global parameters. The choice of μ for a given observable is fixed by the requirement that the $SU(2)_{CS}$ transformations not mix operators with different spin.

The QCD Lagrangian is not invariant under $SU(2)_{CS}$ transformations, but only the chromoelectic part of the quark-gluon interaction, and also the color charge $Q^a = \int d^4x q^\dagger(x)T^a q(x)$. In a given reference frame (e.g., the rest frame of the medium), the quark-gluon interaction in the QCD Lagrangian can be decomposed into temporal and spatial parts:

$$\bar{q}(x)\left\{\gamma_4[\partial_4 + igT^a A_4^a(x)] + \sum_{k=1,2,3}\gamma_k[\partial_k + igT^a A_k^a(x)]\right\}q(x),$$

where the chromoelectric interaction term $igq^\dagger(x)T^a \times A_4^a(x)q(x)$ is invariant under the $SU(2)_{CS}$ transformations, while the chromomagnetic interaction and the kinetic terms break the $SU(2)_{CS}$ symmetry. If the $SU(2)_{CS}$ chiral spin symmetry turns out to be exact for a range of temperatures in high-temperature QCD, then the quarks cannot behave like free fermions at these temperatures, since the latter break the $SU(2)_{CS}$ symmetry. Consequently, it is likely that there are hadron-like objects which are predominantly bound by the chromoelectric interactions into color singlets. On the other hand, if $SU(2)_{CS}$ is an approximate emergent symmetry, then the chromomagnetic interactions could also play some role in forming these hadron-like objects, and the dominance of the chromoelectric interactions depends on to what extent the $SU(2)_{CS}$ symmetry emerges as an exact symmetry.

In the following, we discuss the $SU(2)_{CS}$ multiplets of vector meson correlators, which are generated by the $SU(2)_{CS}$ transformations.

For the t correlators, the choice of $\mu = 4$ satisfies the requirement that the $SU(2)_{CS}$ transformations not mix operators with different spin. Then, the $SU(2)_{CS} \times S_3$ transformations generate one triplet and one nonet:

$$(A_1, A_2, A_3); \quad (V_1, V_2, V_3, T_1, T_2, T_3, X_1, X_2, X_3). \quad (13)$$

For $T \gtrsim T_c^q$, the $SU(2)_L \times SU(2)_R$ chiral symmetry of the flavor doublet (q_1, q_2) is effectively restored (i.e.,

$C_{A_k} = C_{V_k}, k = 1, 2, 3$), and then the triplet and the nonet are degenerate into a single multiplet:

$$(A_1, A_2, A_3, V_1, V_2, V_3, T_1, T_2, T_3, X_1, X_2, X_3). \quad (14)$$

This suggests the possibility of a larger symmetry group $SU(4)$ for $T > T_c^q$ which contains $SU(2)_L \times SU(2)_R \times SU(2)_{CS}$ as a subgroup. For the full $SU(4) \times S_3$ symmetry, the multiplet in Eq. (14) is enlarged to include the flavor-singlet partners of V_k, T_k, and X_k, while the flavor-singlet partners of A_1, A_2, and A_3 are $SU(4)$ singlets—i.e.,

$$(A_1^0, A_2^0, A_3^0); (V_1, V_2, V_3, A_1, A_2, A_3, T_1, T_2, T_3, X_1, X_2, X_3,$$
$$V_1^0, V_2^0, V_3^0, T_1^0, T_2^0, T_3^0, X_1^0, X_2^0, X_3^0), \quad (15)$$

where the superscript "0" denotes the flavor singlet.

For the z correlators, $\mu = 1$ and $\mu = 2$ each satisfy the requirement that the $SU(2)_{CS}$ transformations not mix operators with different spin. Then, the $SU(2)_{CS} \times S_2$ transformations with $\mu = 1$ and $\mu = 2$ together generate the following multiplets:

$$(V_1, V_2); \quad (A_1, A_2, T_4, X_4), \quad (16)$$

$$V_4; \quad (A_4, T_1, T_2, X_1, X_2). \quad (17)$$

For $T \gtrsim T_c^q$, the $SU(2)_L \times SU(2)_R$ chiral symmetry of the (q_1, q_2) doublet is effectively restored, and the multiplets in Eqs. (16) and (17) become two sextets:

$$(V_1, V_2, A_1, A_2, T_4, X_4), \quad (18)$$

$$(V_4, A_4, T_1, T_2, X_1, X_2). \quad (19)$$

This suggests the possibility of a larger symmetry group $SU(4)$ for $T > T_c^q$ which contains $SU(2)_L \times SU(2)_R \times SU(2)_{CS}$ as a subgroup. For the full $SU(4) \times S_2$ symmetry, each of the multiplets in Eqs. (18) and (19) is enlarged to include the flavor-singlet partners of A_k, T_k, and X_k, while the flavor-singlet partners of V_1, V_2, and V_4 are $SU(4)$ singlets—i.e.,

$$(V_1^0, V_2^0); \quad (V_1, V_2, A_1, A_2, T_4, X_4, A_1^0, A_2^0, T_4^0, X_4^0), \quad (20)$$

$$V_4^0; \quad (V_4, A_4, T_1, T_2, X_1, X_2, A_4^0, T_1^0, T_2^0, X_1^0, X_2^0). \quad (21)$$

To investigate the full $SU(4)$ symmetry, it is necessary to examine the degeneracies of the correlators in the multiplets of Eqs. (15), (20), and (21) which involve the flavor singlets. Since the evaluations of the correlators of flavor singlets require the disconnected diagrams which have been omitted in this work, we are not in a position to determine the emergence of the full $SU(4)$ symmetry, even if its subgroup $SU(2)_L \times SU(2)_R \times SU_{CS}(2)$ is manifested approximately due to the effective restoration of

$SU(2)_L \times SU(2)_R$ chiral symmetry and the emergence of approximate $SU(2)_{\mathrm{CS}}$ chiral spin symmetry. Nevertheless, the splittings between the correlators of the flavor singlet and the nonsinglet of u and d quarks are usually very small compared to the correlators of the nonsinglet. Thus, we can envision that the flavor singlets in Eqs. (15), (20), and (21) would be approximately degenerate with all members in the multiplet. In order to justify this, computing the correlators of flavor singlets is indispensible.

To investigate the manifestation of various symmetries from the degeneracies of the t correlators and the z correlators of vector mesons, in view of the S_3 and S_2 symmetries, it suffices to focus on the "1" components of the vector meson correlators (i.e., C_{V_1}, C_{A_1}, C_{T_1}, C_{X_1}, and their flavor-singlet partners), while all "2" and "3" components can be suppressed. With this convention, the multiplets of $SU(2)_{\mathrm{CS}}$ in Eqs. (13), (16), and (17) can be abbreviated as

$$t \text{ correlators: } (A_1); \ (V_1, T_1, X_1), \qquad (22)$$

$$z \text{ correlators: } (V_1); \ (A_1, T_4, X_4), \qquad (23)$$

$$(V_4); \ (A_4, T_1, X_1), \qquad (24)$$

and the degeneracies in the above triplets signal the emergence of $SU(2)_{\mathrm{CS}}$ chiral spin symmetry. Similarly, the $SU(4)$ multiplets in Eqs. (15), (20), and (21) can be abbreviated as

$$t \text{ correlators: } A_1^0; \ (A_1, V_1, T_1, X_1, V_1^0, T_1^0, X_1^0), \qquad (25)$$

$$z \text{ correlators: } V_1^0; \ (V_1, A_1, T_4, X_4, A_1^0, T_4^0, X_4^0), \qquad (26)$$

$$V_4^0; \ (V_4, A_4, T_1, X_1, A_4^0, T_1^0, X_1^0), \qquad (27)$$

and the degeneracies in the above multiplets signal the emergence of $SU(4)$ symmetry.

For $T > T_1^q \gtrsim T_c^q$, the $SU(2)_L \times SU(2)_R$ and $U(1)_A$ chiral symmetries are effectively restored, and $C_{V_k} = C_{A_k}$, $C_{T_k} = C_{X_k}$, $C_{V_k}^0 = C_{A_k}^0$, and $C_{T_k}^0 = C_{X_k}^0$. Thus, to examine the $SU(2)_{\mathrm{CS}}$ symmetry, one only needs to check the degeneracy of the t correlators of (V_1, T_1) in Eq. (22), the degeneracy of the z correlators of (A_1, T_4) in Eq. (23), and the degeneracy of the z correlators of (A_4, T_1) in Eq. (24). Meanwhile, for the $SU(4)$ symmetry, one only needs to check the degenerancy of the t correlators of (V_1, T_1, V_1^0, T_1^0) in Eq. (25), the degeneracy of the z correlators of (A_1, T_4, A_1^0, T_4^0) in Eq. (26), and also of (A_4, T_1, A_4^0, T_1^0) in Eq. (27).

III. SYMMETRY-BREAKING PARAMETERS

In order to give a quantitative measure for the manifestation of symmetries from the degeneracy of temporal/spatial correlators, we consider the symmetry-breaking parameters as follows. To this end, we write the meson correlators as functions of dimensionaless variables

$$tT = (n_t a)/(N_t a) = n_t/N_t, \qquad (28)$$

$$zT = (n_z a)/(N_t a) = n_z/N_t, \qquad (29)$$

where T is the temperature.

A. $U(1)_A$ and $SU(2)_L \times SU(2)_R$ symmetry-breaking parameters

For the $U(1)_A$ symmetry, its breaking in the pseudoscalar (P) and scalar (S) channels can be measured by

$$\kappa_{\mathrm{PS}}(tT) = 1 - \frac{C_S(tT)}{C_P(tT)}, \qquad n_t > 1, \qquad (30)$$

$$\kappa_{\mathrm{PS}}(zT) = 1 - \frac{C_S(zT)}{C_P(zT)}, \qquad n_z > 1, \qquad (31)$$

where C_S and C_P are normalized correlators (with normalization equal to 1 at $n_t = 1$ or $n_z = 1$). If C_P and C_S are exactly degenerate at T, then $\kappa_{\mathrm{PS}} = 0$ for any tT (zT), and the $U(1)_A$ symmetry is effectively restored at T. On the other hand, if there is any discrepancy between C_P and C_S at any tT (zT), then κ_{PS} is nonzero at this tT (zT), and this suggests that $U(1)_A$ is not completely restored at T. Obviously, this criterion is more stringent than the equality of the thermal masses from the temporal correlators as well as the screening masses from the spatial correlators. Similarly, the $U(1)_A$ symmetry breaking in the channels of tensor vectors (T_k) and axial-tensor vectors (X_k) can be measured by

$$\kappa_{\mathrm{TX}}(tT) = 1 - \frac{C_{X_k}(tT)}{C_{T_k}(tT)}, \quad n_t > 1, \quad (k = 1, 2, 3), \quad (32)$$

$$\kappa_{\mathrm{TX}}(zT) = 1 - \frac{C_{X_k}(zT)}{C_{T_k}(zT)}, \quad n_z > 1, \quad (k = 1, 2, 4). \quad (33)$$

Due to the S_3 symmetry of the t correlators, it suffices only to examine the $k = 1$ component in Eq. (32). Similarly, due to the S_2 symmetry of the z correlators, one only needs to examine the $k = 1$ and $k = 4$ components of Eq. (33). In practice, there is no difference between $k = 1$ and $k = 4$ components (up to the statistical uncertainties); thus, the $k = 4$ component is suppressed in the following.

By the same token, the breaking of $SU(2)_L \times SU(2)_R$ chiral symmetry can be measured by

$$\kappa_{\mathrm{VA}}(tT) = 1 - \frac{C_{A_k}(tT)}{C_{V_k}(tT)}, \quad n_t > 1, \quad (k = 1, 2, 3), \quad (34)$$

$$\kappa_{\text{VA}}(zT) = 1 - \frac{C_{A_k}(zT)}{C_{V_k}(zT)}, \quad n_z > 1, \quad (k = 1, 2, 4). \quad (35)$$

If C_{A_k} and C_{V_k} are degenerate, then $\kappa_{\text{VA}} = 0$ for any tT (zT), and the $SU(2)_L \times SU(2)_R$ chiral symmetry is effectively restored. Following the above discussion for κ_{TX}, the components of $k = 2, 3, 4$ in Eqs. (34) and (35) are suppressed.

B. $SU(2)_{\text{CS}}$ symmetry breaking and fading parameters

For the t correlators, the $SU(2)_{\text{CS}}$ symmetry breaking can be measured by the splitting of V_1 and T_1 in the multiplet [Eq. (22)]:

$$\kappa_{\text{AT}}(tT) = \frac{C_{V_1}(tT)}{C_{T_1}(tT)} - 1, \quad n_t > 1, \quad (36)$$

where V_1 and T_1 are connected by the $SU(2)_{\text{CS}}$ transformations. In general, the splitting between $V_1(tT)$ and $T_1(tT)$ is a monotonic decreasing function of T for a fixed tT, and so is $\kappa_{\text{AT}}(tT)$.

As the temperature T is increased, the separation between the multiplets of $SU(2)_{\text{CS}}$ and $U(1)_A$ is decreased. Therefore, at sufficiently high temperatures, the $SU(2)_{\text{CS}} \times SU(2)_L \times SU(2)_R$ multiplet $M_1 = (A_1, V_1, T_1, X_1)$ and the $U(1)_A$ multiplet $M_0 = (P, S)$ merge together, and then the approximate $SU(2)_{\text{CS}}$ symmetry becomes washed out, and only the $U(1)_A \times SU(2)_L \times SU(2)_R$ chiral symmetry remains. The fading of the approximate $SU(2)_{\text{CS}}$ symmetry can be measured by the ratio of the splitting between V_1 and T_1 in the M_1 multiplet to the separation of M_1 and M_0 multiplets:

$$\kappa(tT) = \frac{C_{V_1}(tT) - C_{T_1}(tT)}{C_{M_0}(tT) - C_{M_1}(tT)}, \quad n_t > 1, \quad (37)$$

where

$$C_{M_0}(tT) = \frac{1}{2}[C_P(tT) + C_S(tT)],$$

$$C_{M_1}(tT) = \frac{1}{4}[C_{A_1}(tT) + C_{V_1}(tT) + C_{T_1}(tT) + C_{X_1}(tT)].$$

In general, $\kappa(tT)$ is a monotonic increasing function of T for a fixed tT. If $\kappa(tT) \ll 1$ for a range of T, then the approximate $SU(2)_{\text{CS}}$ symmetry is well defined for this window of T. On the other hand, if $\kappa(tT) \gtrsim 1$ for $T > T_f$, then the approximate $SU(2)_{\text{CS}}$ symmetry becomes washed out, and only the $U(1)_A \times SU(2)_L \times SU(2)_R$ chiral symmetry remains.

Thus, to determine to what extent the $SU(2)_{\text{CS}}$ symmetry is manifested in the t correlators, it is necessary to examine whether both $\kappa(tT)$ and $\kappa_{\text{AT}}(tT)$ are sufficiently small. For a fixed tT, the condition

$$(|\kappa_{\text{AT}}(tT)| < \epsilon_{\text{CS}}) \wedge (|\kappa(tT)| < \epsilon_{\text{CS}}) \quad (38)$$

serves as a criterion for the emergence of approximate $SU(2)_{\text{CS}}$ symmetry in the t correlators, where ϵ_{CS} specifies the precision of $SU(2)_{\text{CS}}$ symmetry. Once ϵ_{CS} is given, the range of temperatures satisfying Eq. (38) can be determined for a fixed tT. Roughly speaking, if there exists a window of temperatures satisfying Eq. (38) with $\epsilon_{\text{CS}} \lesssim 0.01$, then the $SU(2)_{\text{CS}}$ symmetry can be regarded as an exact symmetry emerging in this window. Here, the upper bound 0.01 is estimated based on the maximum values of $\kappa_{\text{PS}}(tT)$, $\kappa_{\text{TX}}(tT)$, and $\kappa_{\text{VA}}(tT)$ among all values of T and tT in this study, as given in Sec. VA. On the other hand, if no temperatures satisfying Eq. (38) exist with $\epsilon_{\text{CS}} < 0.50$, then the $SU(2)_{\text{CS}}$ symmetry can be regarded as not emerging in this theory—e.g., the noninteracting theory with free fermions on the lattice. Otherwise, $0.01 < \epsilon_{\text{CS}} \leq 0.5$, and the $SU(2)_{\text{CS}}$ symmetry can be regarded as an approximate emergent symmetry in this window.

Next, we turn to the $SU(2)_{\text{CS}}$ symmetry-breaking and fading parameters for the z correlators. Note that at sufficiently high temperatures, the $U(1)_A$ multiplet $M_0 = (P, S)$ and the $SU(2)_{\text{CS}} \times SU(2)_L \times SU(2)_R$ multiplet $M_2 = (V_1, A_1, T_4, X_4)$ merge together, and then the approximate $SU(2)_{\text{CS}}$ symmetry becomes washed out, and only the $U(1)_A \times SU(2)_L \times SU(2)_R$ chiral symmetry remains. On the other hand, the $SU(2)_{\text{CS}} \times SU(2)_L \times SU(2)_R$ multiplet $M_4 = (V_4, A_4, T_1, X_1)$ never merges with M_0 and M_2, even in the limit $T \to \infty$ (i.e., the noninteracting theory with free quarks), which can be seen from Eqs. (48) and (49). Thus, the multiplet M_4 is irrelevant to the fading of the approximate $SU(2)_{\text{CS}}$ symmetry.

Now, it is straightforward to transcribe Eqs. (36)–(38) to their counterparts for the z correlators. This gives the $SU(2)_{\text{CS}}$ symmetry-breaking and fading parameters

$$\kappa_{\text{AT}}(zT) = \frac{C_{A_1}(zT)}{C_{T_4}(zT)} - 1, \quad n_z > 1, \quad (39)$$

$$\kappa(zT) = \frac{C_{A_1}(zT) - C_{T_4}(zT)}{C_{M_0}(zT) - C_{M_2}(zT)}, \quad n_z > 1, \quad (40)$$

where

$$C_{M_0}(zT) \equiv \frac{1}{2}[C_P(zT) + C_S(zT)],$$

$$C_{M_2}(zT) \equiv \frac{1}{4}[C_{V_1}(zT) + C_{A_1}(zT) + C_{T_4}(zT) + C_{X_4}(zT)],$$

and the criterion for the emergence of approximate $SU(2)_{\text{CS}}$ symmetry in the z correlators is

$$(|\kappa_{\text{AT}}(zT)| < \epsilon_{\text{CS}}) \wedge (|\kappa(zT)| < \epsilon_{\text{CS}}), \quad (41)$$

where ϵ_{CS} is not necessarily equal to that in Eq. (38). In general, for a fixed zT, $\kappa_{\text{AT}}(zT)$ is a monotonic decreasing

function of T, while $\kappa(zT)$ is a monotonic increasing function of T. Once ϵ_{CS} is given, the range of temperatures satisfying Eq. (41) can be determined for a fixed zT. Note that even for the same ϵ_{CS} and $tT = zT$, the window satisfying Eq. (38) is most likely different from that satisfying Eq. (41). Nevertheless, the classification of the emergent $SU(2)_{CS}$ symmetry as an (exact, approximate, nonexisting) symmetry according to $\epsilon_{CS} = (\leq 0.01, (0.01, 0.5], > 0.5)$ can be used in both cases. Here, the upper bound 0.01 for exact $SU(2)_{CS}$ symmetry is estimated based on the maximum values of $\kappa_{PS}(zT)$, $\kappa_{TX}(zT)$, and $\kappa_{VA}(zT)$ among all values of T and zT in this study, as given in Sec. VI B.

Finally, we note that the $\kappa(tT)$ defined in Ref. [6] for the t correlators can be written as

$$\kappa(tT) = -\frac{C_{V_1}(tT) - C_{T_1}(tT)}{C_S(tT) - C_{V_1}(tT)}, \qquad (42)$$

where the denominator is different from that in Eq. (37). However, for $T > T_1 \gtrsim T_c$, with the effective restoration of $U(1)_A$ and $SU(2)_L \times SU(2)_R$ of u and d quarks, then $C_P = C_S$, $C_{V_1} = C_{A_1}$, and $C_{T_1} = C_{X_1}$. Thus, the difference between the denominators of Eqs. (42) and (37) is equal to $[C_{T_1}(tT) - C_{V_1}(tT)]/2$, which is negligible compared with the denominator $[C_S(tT) - C_{V_1}(tT)]$ itself. Thus, the discrepancy due to two different definitions of $\kappa(tT)$ in Eqs. (42) and (37) is negligible for the meson correlators of u and d quarks, except for an overall minus sign.

Moreover, the $\kappa(zT)$ defined in Ref. [5] for the z correlators can be written as

$$\kappa(zT) = \left| \frac{C_{A_1}(zT) - C_{T_4}(zT)}{C_S(zT) - C_{A_1}(zT)} \right|, \qquad (43)$$

where the denominator is different from that in Eq. (40). Again, for $T > T_1 \gtrsim T_c$, with $C_P = C_S$, $C_{V_1} = C_{A_1}$, and $C_{T_4} = C_{X_4}$, the difference between the denominators of Eqs. (43) and (40) is equal to $[C_{T_4}(zT) - C_{A_1}(zT)]/2$, which is negligible compared with the denominator $[C_S(zT) - C_{A_1}(zT)]$ itself. Thus, the discrepancy due to two different definitions of $\kappa(zT)$ in Eqs. (43) and (40) is negligible for the meson correlators of u and d quarks.

IV. GAUGE ENSEMBLES

The gauge ensembles in this study are generated by hybrid Monte Carlo (HMC) simulation of lattice QCD with $N_f = 2 + 1 + 1$ optimal domain-wall quarks [8] at the physical point, on the $32^3 \times (16, 12, 10, 8, 6, 4)$ lattices, with the plaquette gauge action at $\beta = 6/g^2 = \{6.20, 6.18\}$. This set of ensembles are generated with the same actions [9,10] and algorithms as their counterparts on the $64^3 \times (20, 16, 12, 10, 8, 6)$ lattices [11], but with one-eighth of the spatial volume. The simulations were performed on a GPU cluster of 32 nodes (64 GPUs) with various Nvidia GPUs consisting of GTX-970/1060/1070/1080 and TITAN-X. The initial thermalization of each ensemble was performed in one node with one GPU or two GPUs with peer-to-peer communication via the PCIe bus. The initial thermalization of each ensemble was performed in one node with 1–2 GPUs. After thermalization, a set of gauge configurations were sampled and distributed to 16–32 simulation units, and each unit (1–2 GPUs) performed an independent stream of HMC simulation. For each HMC stream, one configuration was sampled for every five trajectories. Finally, collecting all sampled configurations from all HMC streams gives the total number of configurations of each ensemble. The lattice parameters and statistics of the gauge ensembles for computing the meson correlators in this study are summarized in Table II. The temperatures of these six ensembles are in the range ~190–770 MeV, all above the pseudocritical temperature $T_c \sim 150$ MeV.

The lattice spacing and the $(u/d, s, c)$ quark masses are determined on the $32^3 \times 64$ lattices, with the number of configurations (221,292) for $\beta = (6.18, 6.20)$, respectively. The lattice spacing is determined using the Wilson flow [12,13] with the condition $\{t^2 \langle E(t) \rangle\}|_{t=t_0} = 0.3$ and the input $\sqrt{t_0} = 0.1416(8)$ fm [14]. The physical $(u/d, s, c)$ quark masses are obtained by tuning their masses such that the masses of the lowest-lying states extracted from the time-correlation functions of the meson operators $\{\bar{u}\gamma_5 d, \bar{s}\gamma_i s, \bar{c}\gamma_i c\}$ are in good agreement with the physical masses of $\pi^{\pm}(140)$, $\phi(1020)$, and $J/\psi(3097)$.

The chiral symmetry breaking due to finite $N_s = 16$ (in the fifth dimension) can be measured by the residual mass

TABLE II. The lattice parameters and statistics of the six gauge ensembles for computing the meson correlators. The last three columns are the residual masses of u/d, s, and c quarks.

β	a[fm]	N_x	N_t	$m_{u/d}a$	$m_s a$	$m_c a$	T[MeV]	N_{confs}	$(m_{u/d}a)_{\text{res}}$	$(m_s a)_{\text{res}}$	$(m_c a)_{\text{res}}$
6.20	0.0641	32	16	0.00125	0.040	0.550	193	583	$1.9(2) \times 10^{-5}$	$1.5(2) \times 10^{-5}$	$4.3(7) \times 10^{-6}$
6.18	0.0685	32	12	0.00180	0.058	0.626	240	781	$1.9(2) \times 10^{-5}$	$1.6(1) \times 10^{-5}$	$3.8(5) \times 10^{-6}$
6.20	0.0641	32	10	0.00125	0.040	0.550	307	481	$5.7(7) \times 10^{-6}$	$5.1(6) \times 10^{-6}$	$1.4(2) \times 10^{-6}$
6.20	0.0641	32	8	0.00125	0.040	0.550	384	468	$6.3(9) \times 10^{-6}$	$6.0(7) \times 10^{-6}$	$3.0(9) \times 10^{-6}$
6.20	0.0641	32	6	0.00125	0.040	0.550	512	431	$5.8(9) \times 10^{-6}$	$5.6(8) \times 10^{-6}$	$3.4(7) \times 10^{-6}$
6.20	0.0641	32	4	0.00125	0.040	0.550	768	991	$1.2(2) \times 10^{-6}$	$1.2(2) \times 10^{-6}$	$1.2(2) \times 10^{-6}$

of each quark flavor [15], as given in the last three columns of Table II. The residual masses of $(u/d, s, c)$ quarks are less than $(1.5\%, 0.04\%, 0.001\%)$ of their bare masses, amounting to less than $(0.06, 0.05, 0.02)$ MeV/c^2, respectively. This asserts that the chiral symmetry is well preserved, such that the deviation of the bare quark mass m_q is sufficiently small in the effective 4D Dirac operator of optimal DWF, for both light and heavy quarks. In other words, the chiral symmetry in the simulations is sufficiently precise to guarantee that the hadronic observables (e.g., meson correlators) can be evaluated to high precision, with the associated uncertainty being much less than those due to statistics and other systematics.

V. TEMPORAL CORRELATORS OF $\bar{u}\Gamma d$

A. Results of $N_f = 2 + 1 + 1$ lattice QCD

In the left panels of Fig. 1, the temporal correlators of $\bar{u}\Gamma d$ are plotted as a function of the dimensionless variable tT [Eq. (28)]. Each panel displays the normalized t correlators (with the normalization equal to 1 at $n_t = 1$) for all meson interpolators (see Table I), for n_t from 1 to $N_t/2$. Due to the degeneracy (the S_3 symmetry) of the "1," "2," and "3" components in the t correlators of $J = 1$ mesons, only the "1" components are plotted in Fig. 1.

For the three temperatures in the range $T \sim 190 - 310$ MeV, the $U(1)_A$ symmetry seems to be effectively restored, as shown by the degeneracies $C_P(t) = C_S(t)$ and $C_{T_1}(t) = C_{X_1}(t)$. Moreover, the $SU(2)_L \times SU(2)_R$ chiral symmetry is also effectively restored, as shown by the degeneracy $C_{V_1}(t) = C_{A_1}(t)$.

Due to the effective restoration of $U(1)_A$ and $SU(2)_L \times SU(2)_R$ chiral symmetries, in each left panel of Fig. 1, there emerge three distinct multiplets: (P, S), (V_1, A_1), and (T_1, X_1). They appear in the order

$$C_{P,S} > C_{V_1,A_1} > C_{T_1,X_1}, \quad \text{for } n_t > 1, \qquad (44)$$

which is consistent with $N_f = 2 + 1 + 1$ lattice QCD at $T < T_c \sim 150$ MeV.

As the temperature T is increased from 193 MeV to 307 MeV, the multiplets (V_1, A_1) and (T_1, X_1) tend to merge together to form a single multiplet $M_1 = (A_1, V_1, T_1, X_1)$, in agreement with the $SU(2)_{CS}$ multiplets [Eq. (22)] and the $SU(4)$ multiplet [Eq. (25)]. This suggests the emergence of approximate $SU(2)_{CS}$ and $SU(4)$ symmetries. Moreover, we observe that the separation between M_1 and the $U(1)_A$ multiplet $M_0 = (P, S)$ becomes smaller and smaller as T is increased from 193 MeV to 307 MeV. Therefore, at sufficiently high temperatures above 307 MeV—say, $T \geq T_f$—M_1 and M_0 would merge together, and then the approximate $SU(2)_{CS}$ and $SU(4)$ symmetries become washed out, and only the $U(1)_A \times SU(2)_L \times SU(2)_R$ chiral symmetry remains. In other words, the approximate $SU(2)_{CS}$ and $SU(4)$ symmetries

can only appear in a range of temperatures above T_c—say $T_c < T_{CS} \lesssim T \lesssim T_f$—where T_{CS} and T_f depend on the ϵ_{CS} in the criterion [Eq. (38)] for the emergence of approximate $SU(2)_{CS}$ symmetry in the t correlators.

Next, we examine the symmetries in the temporal correlators with the symmetry-breaking parameters as defined by κ_{PS} [Eq. (30)], κ_{TX} [Eq. (32)], κ_{VA} [Eq. (34)], κ_{AT} [Eq. (36)], and κ [Eq. (37)] in Sec. III. In Fig. 1, the symmetry-breaking parameters are plotted in the right panels, with one-to-one correspondence to the t correlators in the left panels.

For all three temperatures in the range $T \sim 190 - 310$ MeV, the $SU(2)_L \times SU(2)_R$ chiral symmetry is effectively restored with the maximum value of κ_{VA} equal to $5.2(8) \times 10^{-4}$ at $T \sim 193$ MeV and $tT = 0.5$.

For the $U(1)_A$ symmetry, there are tiny breakings at $T = 193$ MeV and $tT = 0.5$ with the maximum value of κ_{TX} equal to $3.5(5) \times 10^{-3}$, while that of κ_{PS} is equal to $2.1(3) \times 10^{-2}$. This seems to suggest that the effective restoration of $U(1)_A$ symmetry occurs at temperatures higher than 193 MeV. To confirm or refute this requires us to determine κ_{PS} and κ_{TX} in the continuum limit, which is beyond the scope of this paper.

For the $SU(2)_{CS}$ chiral spin symmetry, it turns out to be a rather approximate symmetry in comparison with the $U(1)_A$ and $SU(2)_L \times SU(2)_R$ chiral symmetries, as shown in the right panels of Fig. 1. Also, this can be seen by plotting κ_{AT} and κ versus the temperature T, for $tT = 0.50$ and $tT = 0.25$, as shown in Fig. 2. Here, the data points at $T = 307$ MeV ($N_t = 10$) for $tT = 0.25$ are obtained by interpolation between $tT = 0.2$ and $tT = 0.3$. For $tT = 0.5$, κ_{AT} is decreased from 0.34(3) to 0.21(2) to 0.04(2) as T is increased from 193 MeV to 307 MeV, while κ is changed from 0.056(4) to 0.08(1) to 0.04(3). The last data point of κ at $T = 307$ MeV looks exceptional. Presumably, for any fixed tT, κ is a monotonic increasing function of T. It is unknown why the data of κ at $T = 307$ MeV are not a clean cut. It could be just due to the finite-size effects of the small $N_t = 10$ in the temporal direction. Further investigations are needed to clarify this. For $tT = 0.25$, κ_{AT} is decreased from 0.50(1) to 0.36(1) to 0.21(1) as T is increased from 193 MeV to 307 MeV, while κ is increased from 0.170(4) to 0.26(1) to 0.34(2).

Now, using the data of κ_{AT} and κ as plotted in Fig. 2 and the criterion in Eq. (38), the ranges of temperatures for the emergence of approximate $SU(2)_{CS}$ symmetry can be determined, as tabulated in Table III, for $tT = (0.5, 0.25)$ and $\epsilon_{CS} = (0.20, 0.10, 0.05, 0.03)$.

For $tT = 0.5$ in the second column of Table III, the lower bound of T is increased as the ϵ_{CS} is decreased, and then at $\epsilon_{CS} = 0.03$, the window is shrunk to zero. The upper bounds of the window for $\epsilon_{CS} = (0.20, 0.10, 0.05)$ are T_x, T_y, and T_z, which have yet to be determined. The fact that the window is shrunk to zero for $\epsilon_{CS} \leq 0.03$ implies that the
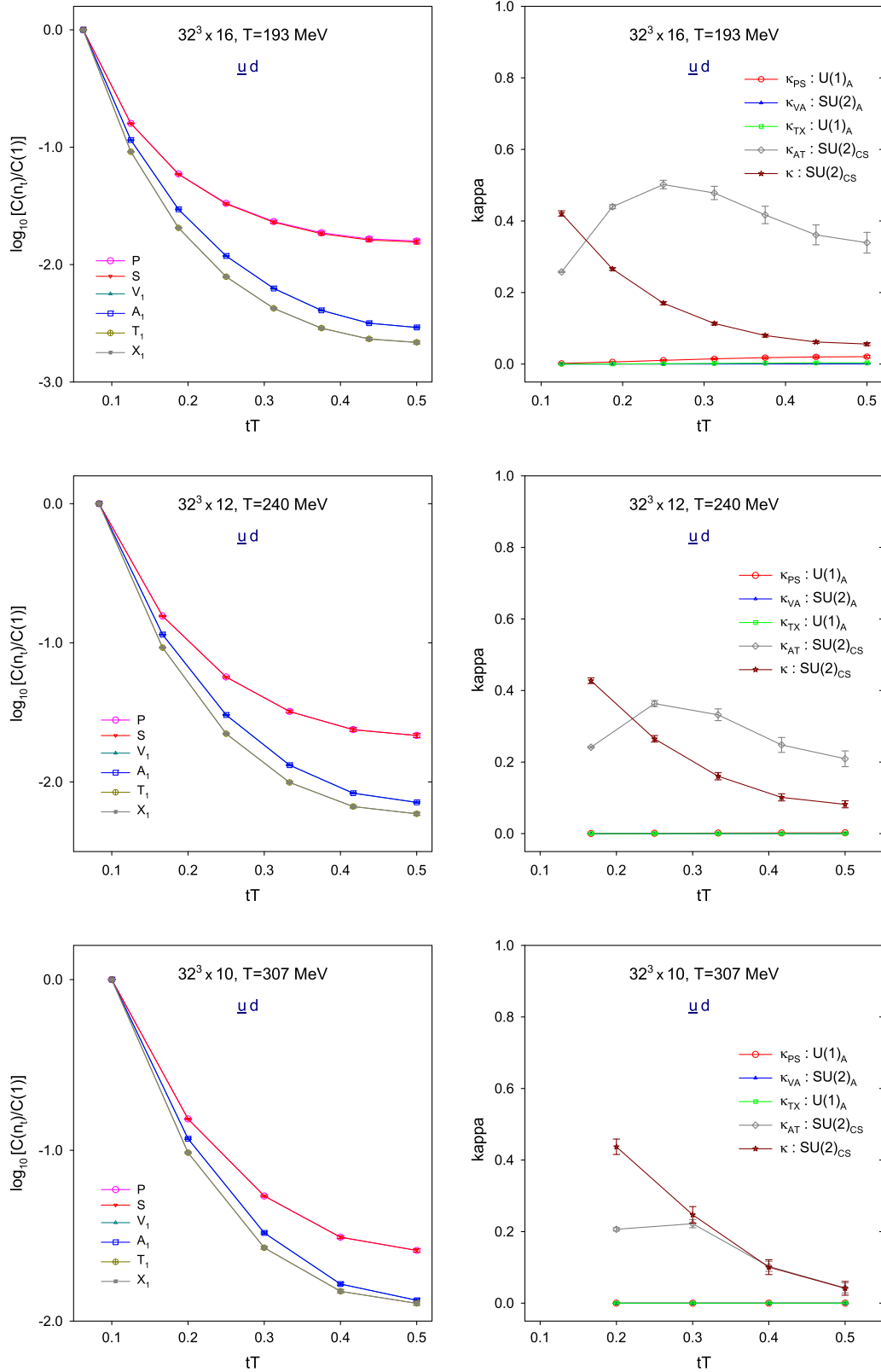
FIG. 1. The left panels are the normalized t correlators of $\bar{u}\Gamma d$ in $N_f = 2+1+1$ lattice QCD at the physical point for $T = (193, 240, 307)$ MeV, while the right panels are the symmetry-breaking parameters corresponding to the left panels.
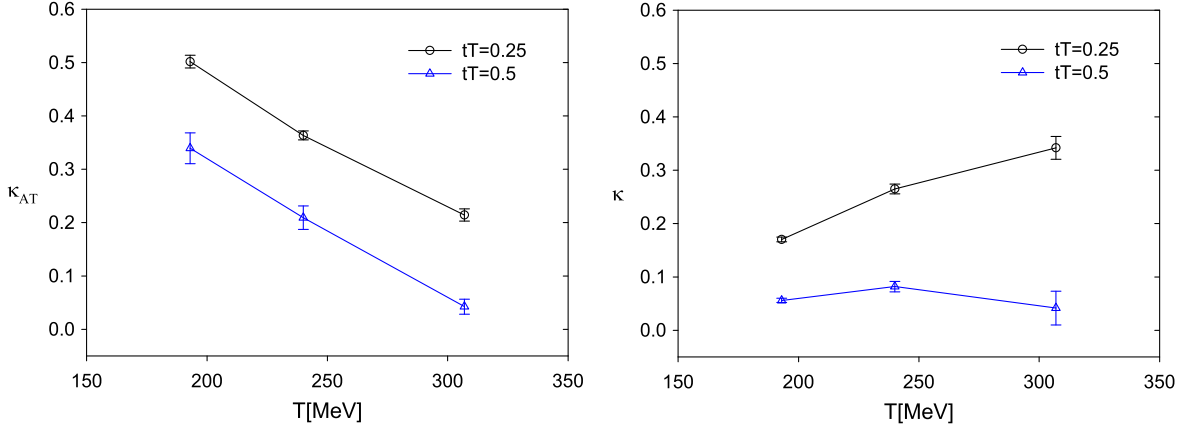
FIG. 2. The $SU(2)_{CS}$ symmetry-breaking and fading parameters (κ_{AT}, κ) in $N_f = 2 + 1 + 1$ lattice QCD at the physical point, for $tT = (0.5, 0.25)$ and $T = (193, 240, 307)$ MeV.

$SU(2)_{CS}$ symmetry of the temporal correlators of u and d quarks in $N_f = 2 + 1 + 1$ lattice QCD is at most an approximate emergent symmetry, which never becomes an exact symmetry, unlike the $U(1)_A \times SU(2)_L \times SU(2)_R$ chiral symmetry, which is effectively restored as an exact symmetry for $T > T_1 \gtrsim T_c$.

For $tT = 0.25$ in the third column of Table III, there are no temperatures satisfying the criterion [Eq. (38)] with $\epsilon_{CS} \le 0.20$. Note that the t correlators at $tT = 0.25$ (with a small t) have large contributions from the excited states; thus, they may not suitable for the criterion of Eq. (38).

B. Comparison with the noninteracting theory

The t correlators of $\bar{u}\Gamma d$ constructed with free-quark propagators are plotted in the left panels of Fig. 3. The free-quark propagators are computed with the same boundary conditions, the same lattice size, and the same u/d quark masses as those in $N_f = 2 + 1 + 1$ QCD, but with all link variables equal to the identity matrix. Note that the lattice spacing a and the temperature $T = 1/(N_t a)$ are not defined for the free quarks. Thus, the label tT of the horizontal axis in Fig. 3 should be regarded as $tT = n_t/N_t$. In the following, the temperature T for all quantities with free quarks is always understood to be the corresponding temperature $T = 1/(N_t a)$ in $N_f = 2 + 1 + 1$ lattice QCD with the same N_t.

TABLE III. The approximate ranges of temperatures satisfying the criterion in Eq. (38) with $\epsilon_{CS} = (0.20, 0.10, 0.05, 0.03)$ for $tT = (0.5, 0.25)$. In the second column ($tT = 0.5$), T_x, T_y, and T_z have yet to be determined.

ϵ_{CS}	$tT = 0.5$	$tT = 0.25$
0.20	~244 MeV$-T_x$	NULL
0.10	~280 MeV$-T_y$	NULL
0.05	~304 MeV$-T_z$	NULL
0.03	NULL	NULL

In the left panels of Fig. 3, for all three lattice sizes $32^3 \times (16, 12, 10)$, the $U(1)_A \times SU(2)_L \times SU(2)_R$ chiral symmetry is almost exact in spite of the nonzero u/d quark masses, as shown by the degeneracies $C_P(t) = C_S(t)$, $C_{T_1}(t) = C_{X_1}(t)$, and $C_{V_1}(t) = C_{A_1}(t)$. Consequently, it appears that there are only three distinct t correlators in each left panel of Fig. 3. They are in the order of

$$C_{P,S}(\text{free}) > C_{V_1,A_1}(\text{free}) > C_{T_1,X_1}(\text{free}),$$
$$\text{for } 1 < n_t < N_t/4, \tag{45}$$

$$C_{P,S}(\text{free}) < C_{V_1,A_1}(\text{free}) < C_{T_1,X_1}(\text{free}),$$
$$\text{for } n_t \ge N_t/4, \tag{46}$$

which is different from the order [Eq. (44)] of the $N_f = 2 + 1 + 1$ lattice QCD at $T \sim 190$–310 MeV.

Next, we examine the symmetries in the t correlators of free quarks with the symmetry-breaking parameters, as defined in Sec. III. In the right panels of Fig. 3, the symmetry-breaking parameters are plotted versus $tT = n_t/N_t$ for $N_t = (16, 12, 10)$. For $U(1)_A$ and $SU(2)_L \times SU(2)_R$ chiral symmetries, $\kappa_{PS} \simeq \kappa_{TX} \simeq \kappa_{VA} < 10^{-6}$, which shows that the $U(1)_A \times SU(2)_L \times SU(2)_R$ chiral symmetry is almost exact in the noninteracting theory with free quarks, in spite of the nonzero u/d quark masses. For the $SU(2)_{CS}$ symmetry, the symmetry-breaking and fading parameters $\kappa_{AT}(tT)$ and $\kappa(tT)$ are much larger than those $(\kappa_{PS}, \kappa_{TX}, \text{and } \kappa_{VA})$ of the $U(1)_A$ and $SU(2)_L \times SU(2)_R$ chiral symmetries. Since $\kappa(tT) \gtrsim 1$ for any $tT = n_t/N_t$ and N_t, there does not exist any N_t satisfying the criterion of Eq. (38) with $\epsilon_{CS} < 1$. Thus, the $SU(2)_{CS}$ symmetry does not emerge in the noninteracting theory on a lattice, in contrast to the $N_f = 2 + 1 + 1$ lattice QCD at the physical point, with the emergence of approximate $SU(2)_{CS}$ symmetry in the windows, as tabulated in Table III. This implies that u and d quarks at these temperatures must be
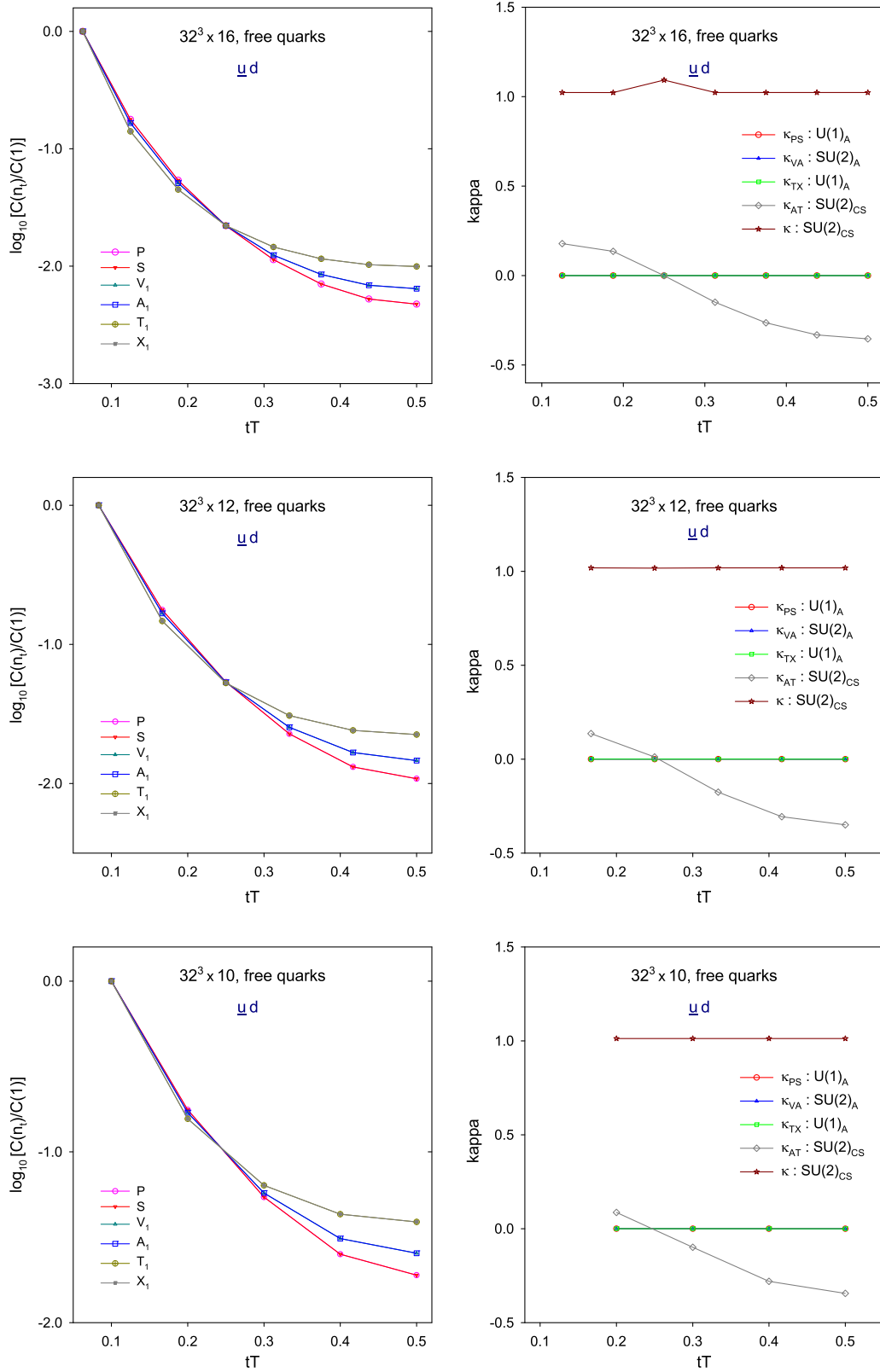
FIG. 3.   The left panels are t correlators of $\bar{u}\Gamma d$ constructed by the free-quark propagators (see text for details). The right panels are the symmetry-breaking parameters (κ_{PS}, κ_{TX}, κ_{VA}, κ_{AT}, and κ) corresponding to the t correlators in the left panels.

dynamically very different from the free or quasifree fermions. If the deconfined quarks in high-temperature QCD behave like free or quasifree fermions, then the u and d quarks in $N_f = 2 + 1 + 1$ lattice QCD at the temperatures with approximate $SU(2)_{CS}$ emergent symmetry are likely to be confined inside hadron-like objects, which are predominantly bound by the chromoelectric interactions into color singlets. Moreover, since the emergent $SU(2)_{CS}$ symmetry is not an exact symmetry, the role of chromomagnetic interactions in forming these hadron-like objects cannot be neglected.

C. Comparison with the $N_f = 2$ lattice QCD

In Ref. [6], the symmetries of temporal correlators of $\bar{u}\Gamma d$ were studied in $N_f = 2$ lattice QCD at $T = 220$ MeV with Möbius domain-wall fermions, on the $48^3 \times 12$ lattice with lattice spacing $a = 0.075$ fm.

Comparing the t correlators of $N_f = 2 + 1 + 1$ lattice QCD at $T = 240$ MeV (in the middle-left panel of Fig. 1) with those of $N_f = 2$ lattice QCD at $T = 220$ MeV [6], we see that in both cases, the order of Eq. (44) is satisfied, and $U_A(1)$ and $SU(2)_L \times SU(2)_R$ chiral symmetries are effectively restored. However, the $SU(2)_{CS}$ symmetry breakings in $N_f = 2 + 1 + 1$ lattice QCD are larger than those in $N_f = 2$ lattice QCD. This can be seen from the approximately degenerate multiplets (V_1, A_1) and (T_1, X_1) in the middle-left panel of Fig. 1 versus the highly degenerate multiplets (V_1, A_1) and (T_1, X_1) in the right panel of Fig. 2 in Ref. [6]. Consequently, the values of κ_{AT} [Eq. (36)] of $N_f = 2 + 1 + 1$ lattice QCD (as shown in the middle-right panel of Fig. 1) are larger than their counterparts of $N_f = 2$ lattice QCD (which are not shown explicitly in Ref. [6]).

Next, we compare the $SU(2)_{CS}$ symmetry-fading parameter κ [Eq. (37)] between $N_f = 2 + 1 + 1$ and $N_f = 2$ lattice QCD. In Fig. 4, the values of κ are plotted for
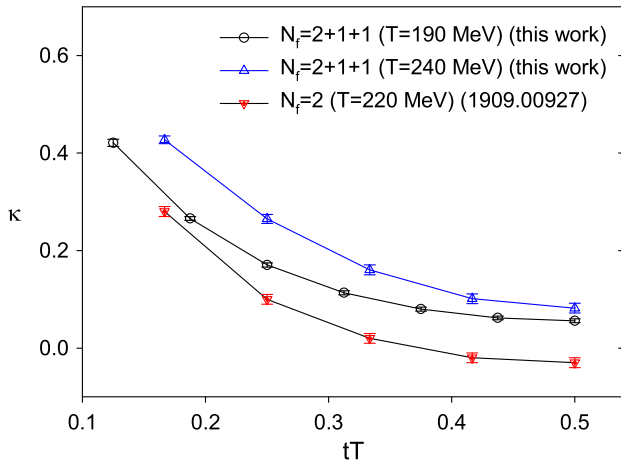

FIG. 4. Comparision of the $SU(2)_{CS}$ symmetry-fading parameter κ between $N_f = 2 + 1 + 1$ lattice QCD at $T = (193, 240)$ MeV (this work) and $N_f = 2$ lattice QCD at $T = 220$ MeV [6].

$N_f = 2$ lattice QCD at $T = 220$ MeV [which are read off from Fig. 3 of Ref. [6], after multiplying by (-1) due to different definitions of κ], and also for $N_f = 2 + 1 + 1$ lattice QCD at $T = (193, 240)$ MeV (same as the values of κ in the right panels of Fig. 1). Evidently, the κ values of $N_f = 2 + 1 + 1$ lattice QCD at $T = (193, 240)$ MeV are larger than those of $N_f = 2$ lattice QCD at $T = 220$ MeV.

VI. SPATIAL CORRELATORS OF $\bar{u}\Gamma d$

A. The issue of unphysical meson states and its resolution

In Fig. 5, the normalized z correlators of $\bar{u}\Gamma d$ (see Table I) at $T = 193$ MeV are plotted in the left panel, while their counterparts constructed with the free-quark propagators are plotted in the right panel. Here, the normalized z correlators are plotted as a function of the dimensionless variable zT [Eq. (29)]. Due to the degeneracy (the S_2 symmetry) of the "1" and "2" components in the z correlators of vector meson interpolators, only the "1" components are plotted.

We note that C_{V_4,A_4} and C_{T_1,X_1} at large distances with $n_z \geq 12$ are seriously distorted by the contribution of unphysical meson states, which have the opposite sign from physical meson states. Consequently, the cancellation between the contributions of the physical and the unphysical meson states produces large statistical errors for C_{V_4,A_4} and C_{T_1,X_1} at $n_z \geq 12$. In the case of free quarks, the issue of unphysical meson states is even more serious, as shown in the right panel of Fig. 5, in which $C_{V_4,A_4} < 0$ for $n_z \geq 12$, and $C_{T_1,X_1} < 0$ for $n_z \geq 11$. The issue due to the unphysical meson states is also visible in the meson spatial correlators of $N_f = 2$ lattice QCD [5], and it was discussed in Ref. [16].

The unphysical meson states are essentially due to the superposition of $+\hat{z}$ (forward) and $-\hat{z}$ (backward) running quark propagators, which are nothing but the finite size effects. Since the unphysical meson states change sign if the boundary condition in the z direction is changed from periodic to antiperiodic, this leads to the following prescription for eliminating the contribution of unphysical meson states to the spatial z correlators:

First, we compute two sets of quark propagators with periodic and antiperiodic boundary conditions in the z direction, while their boundary conditions in the (x, y, t) directions are the same: i.e., periodic in the (x, y) directions, and antiperiodic in the t direction. Each set of quark propagators is used to construct the z correlators independently, and we finally take the average of these two z correlators. Then, the contribution of unphysical meson states to the z correlators can be cancelled configuration by configuration, up to the numerical precision of the quark propagators. Using this prescription, the averaged z correlators of $\bar{u}\Gamma d$ at $T = 193$ MeV are plotted in the left panel of Fig. 6, while their counterparts constructed with the
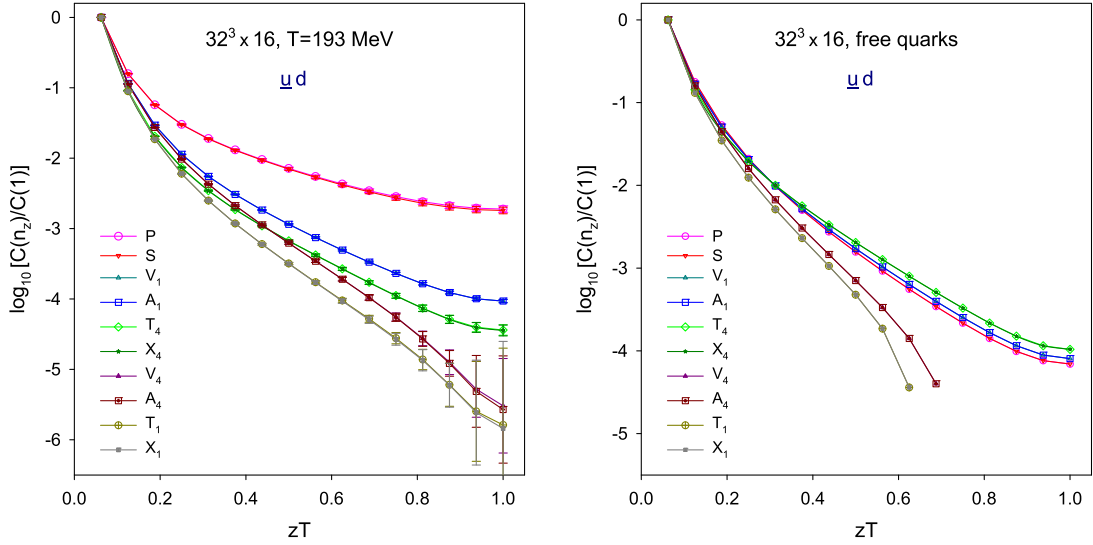
FIG. 5. The normalized z correlators of meson interpolators $\bar{u}\Gamma d$ on the $32^3 \times 16$ lattice at $T = 193$ MeV (left panel), and their counterparts constructed with the free-quark propagators (right panel). The quark propagators are computed with periodic boundary conditions in the (x, y, z) directions and an antiperiodic boundary condition in the t direction.
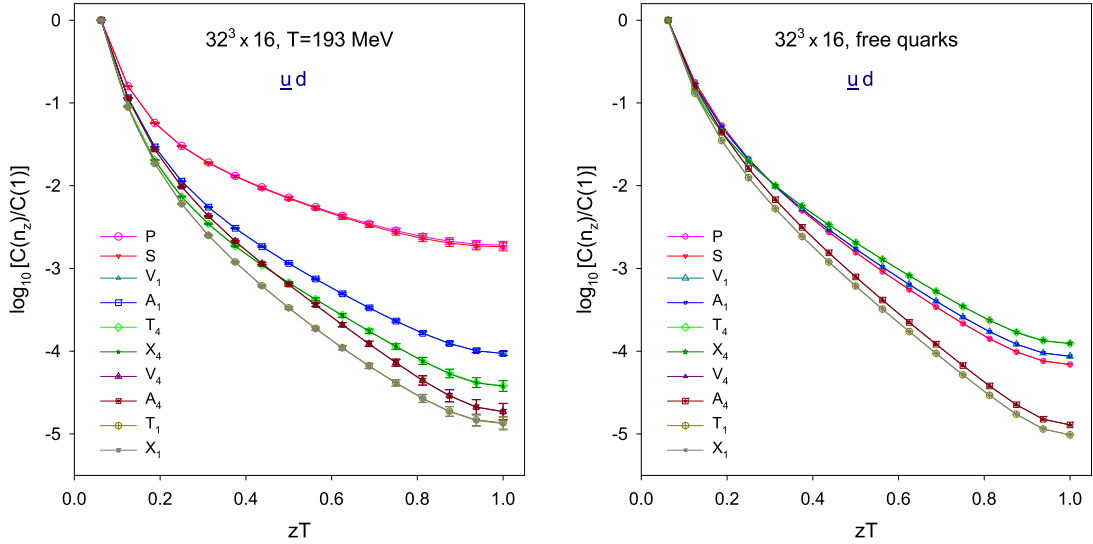

FIG. 6. The contribution of unphysical meson states to the z correlators in Fig. 5 are eliminated with the proposed precription. Here, each z correlator is the average of two z correlators constructed from two sets of quark propagators with periodic and antiperiodic boundary conditions in the z direction. (See text for details.)

free-quark propagators are plotted in the right panel. Evidently, the contributions of unphysical meson states are eliminated in both $N_f = 2 + 1 + 1$ lattice QCD and the noninteracting theory with free quarks. Note that there is another viable prescription for eliminating the unphysical meson states, which will be discussed in Sec. VII.

B. Results of $N_f = 2 + 1 + 1$ lattice QCD

In the following section, for the spatial z correlators, we always use the average of two z correlators constructed from two sets of quark propagators with periodic and

antiperiodic boundary conditions in the z direction. In each panel of Fig. 7, the normalized z correlators of $\bar{u}\Gamma d$ (see Table I) are plotted as a function of the dimensionless variable zT [Eq. (29)]. Due to the degeneracy (the S_2 symmetry) of the "1" and "2" components in the z correlators of vector mesons, only the "1" components are plotted.

For all six temperatures in the range $T \sim 190$–770 MeV, the $SU(2)_L \times SU(2)_R$ chiral symmetry is effectively restored, as manifested in the degeneracy $C_{V_1}(z) = C_{A_1}(z)$. Moreover, the $U(1)_A$ symmetry is effectively restored, as manifested in the degeneracies $C_P(z) = C_S(z)$
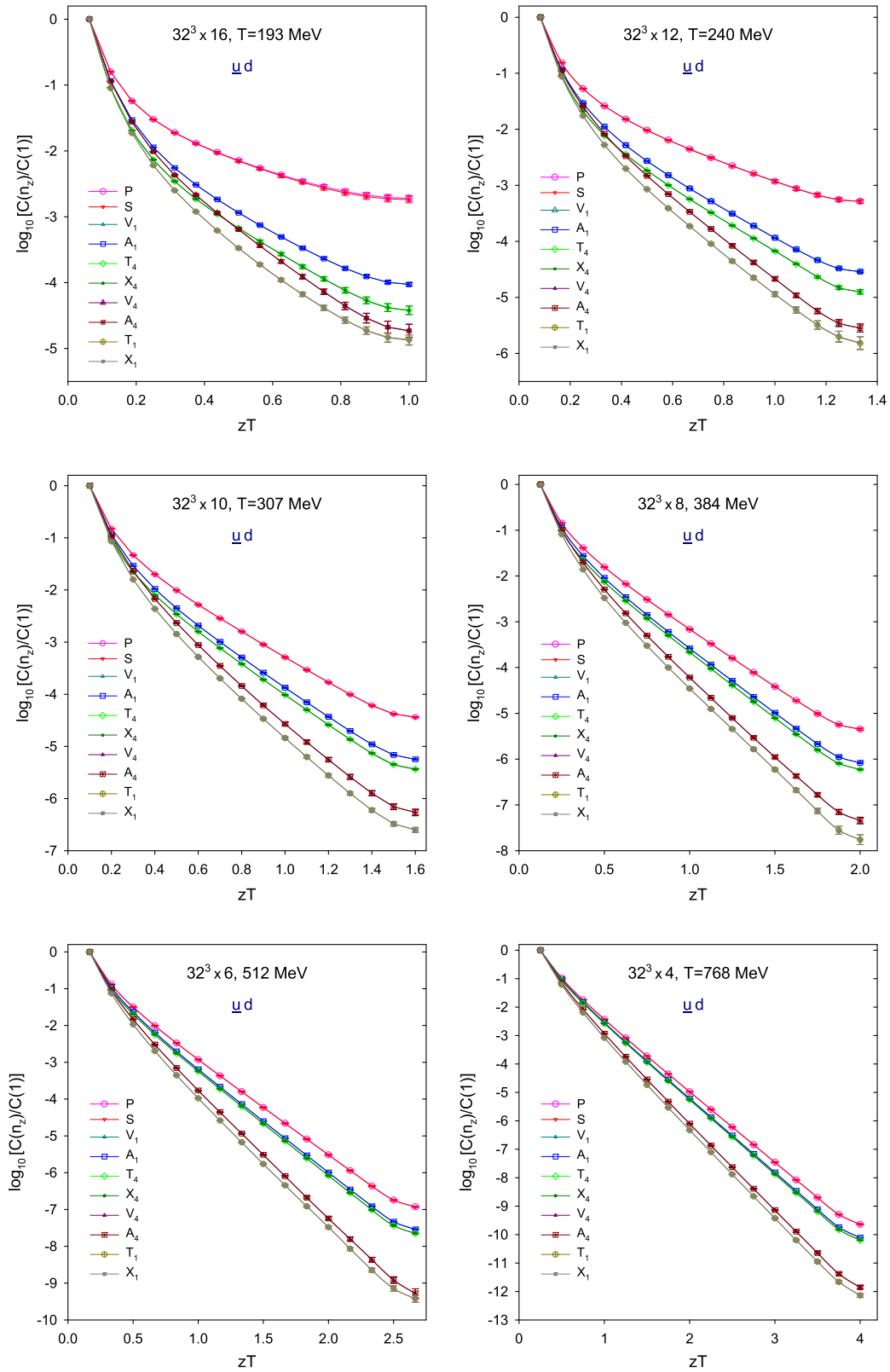
FIG. 7. The spatial z correlators of $\bar{u}\Gamma d$ in $N_f = 2 + 1 + 1$ lattice QCD for $T \simeq 190$–770 MeV.

(except for the small breakings at large z at $T = 193$ MeV) and $C_{T_1}(z) = C_{X_1}(z)$.

Due to the effective restoration of $U(1)_A$ and $SU(2)_L \times SU(2)_R$ chiral symmetries, it appears that there are only five distinct z correlators in each panel of Fig. 7. They are in the order

$$C_{P,S} > C_{V_1,A_1} > C_{T_4,X_4} > C_{V_4,A_4} > C_{T_1,X_1}, \quad \text{for } n_z \geq 7. \quad (47)$$

Note that there is a "level crossing" in the channels of (T_4, X_4) and (V_4, A_4) at $T = 193$ MeV: namely, $C_{T_4,X_4} < C_{V_4,A_4}$ for $1 < n_z \leq 7$, while $C_{T_4,X_4} > C_{V_4,A_4}$ for $n_z > 7$.

As the temperature is increased from 193 MeV to 768 MeV, we see the emergence of three distinct multiplets,

$$M_0 = (P, S),$$
$$M_2 = (V_1, A_1, T_4, X_4),$$
$$M_4 = (V_4, A_4, T_1, X_1),$$

which become more pronounced at higher temperatures. Note that the emergence of the multiplets M_2 and M_4 is in agreement with the $SU(2)_{CS}$ multiplets [Eqs. (16) and (17)] and the $SU(4)$ multiplets [Eqs. (20) and (21)]. This suggests the emergence of the approximate $SU(2)_{CS}$ and $SU(4)$ symmetries for $T \sim 380$–770 MeV. Moreover, the splitting between the multiplets M_2 and M_0 is decreased as the temperature is increased. Thus, at sufficiently high temperatures, M_2 and M_0 would merge together to form a single multiplet, and then the approximate $SU(2)_{CS}$ and $SU(4)$ symmetries become washed out, and only the $U(1)_A \times SU(2)_L \times SU(2)_R$ chiral symmetry remains. In other words, the approximate $SU(2)_{CS}$ and $SU(4)$ symmetries can only appear in a range of temperatures above T_c—say $T_c < T_{CS} \lesssim T \lesssim T_f$—where T_{CS} and T_f depend on the ϵ_{CS} in the criterion [Eq. (41)] for the emergence of approximate $SU(2)_{CS}$ symmetry in the z correlators.

Note that the multiplet M_4 never merges with the multiplets M_0 and M_2, even in the limit $T \to \infty$ (the noninteracting theory with free quarks). This can be seen as follows. In the noninteracting theory, the z correlators of M_4 have different asymptotic behaviors from those of M_0 and M_2—namely,

$$\lim_{z \to \infty} C_{P,S,V_1,A_1,T_4,X_4}(z) \to c_0 \frac{e^{-2\pi zT}}{z}, \quad (48)$$

$$\lim_{z \to \infty} C_{V_4,A_4,T_1,X_1}(z) \to c_4 \frac{e^{-2\pi zT}}{z^2}, \quad (49)$$

where c_0 and c_4 are fixed by the normalization $C_\Gamma(n_z = 1) = 1$. Evidently, Eq. (49) never merges with Eq. (48), which can be easily seen by plotting $\log[C_\Gamma(z)]$ versus z. Thus, turning on the QCD interactions must make M_4 further apart from M_0 and M_2.

Next, we examine the symmetries in the spatial correlators with the symmetry-breaking parameters as defined by Eqs. (31), (33), (35), (39), and (40) in Sec. III. In Fig. 8, the symmetry-breaking parameters κ_{PS}, κ_{VA}, κ_{TX}, κ_{AT}, and κ corresponding to Fig. 7 are plotted versus zT, for temperatures $T \sim 193$–768 MeV.

For all six temperatures in the range $T \sim 193$–768 MeV, the $SU(2)_L \times SU(2)_R$ chiral symmetry is effectively restored with the maximum value of κ_{VA} equal to $8.7(4) \times 10^{-4}$ at $T \sim 193$ MeV and $zT = 0.75$.

For the $U(1)_A$ symmetry, there are tiny breakings (especially at large z) at $T \sim 193$ MeV with the maximum value of κ_{TX} equal to $8.7(8) \times 10^{-3}$ at $zT = 0.6875$, while that of κ_{PS} is equal to $5.1(6) \times 10^{-2}$ at $zT = 0.8125$. Therefore, it seems that κ_{PS} and κ_{TX} give incompatible answers at $T \sim 193$ MeV (similar to their counterparts in the t correlators, as shown in the top-right panel of Fig. 1), and this also suggests that the effective restoration of $U(1)_A$ symmetry is likely to occur at temperatures higher than 193 MeV. To confirm or refute this, it is necessary to determine κ_{PS} and κ_{TX} in the continuum limit, which is beyond the scope of this paper.

For the $SU(2)_{CS}$ symmetry, the symmetry-breaking and -fading parameters $\kappa_{AT}(zT)$ and $\kappa(zT)$ are much larger than those (κ_{PS}, κ_{TX}, and κ_{VA}) of the $U(1)_A$ and $SU(2)_L \times SU(2)_R$ chiral symmetries, as shown in Fig. 8.

In Fig. 9, $\kappa_{AT}(zT)$ and $\kappa(zT)$ are plotted versus the temperature T, for $zT = (0.5, 1, 2)$. In general, for any fixed zT, κ_{AT} is a monotonic decreasing function of T, while κ is a monotonic increasing function of T.

Using the data of κ_{AT} and κ in Fig. 9 and the criterion in Eq. (41) for the emergence of approximate $SU(2)_{CS}$ symmetry, the range of temperatures satisfying Eq. (41) can be determined for any zT and ϵ_{CS}. In Table IV, the ranges of temperatures satisfying Eq. (41) with $\epsilon_{CS} = (0.20, 0.10, 0.05)$ are tabulated for $zT = (2.0, 1.0, 0.5)$. Note that for $zT = 2$, the upper bounds of the windows, $T_x(> 770$ MeV) and $T_y(> 770$ MeV), have not yet been determined, since the highest temperature in this study is ~ 770 MeV. In general, for any fixed zT, the window of temperatures is shrunk as ϵ_{CS} is decreased [i.e., a more precise $SU(2)_{CS}$ symmetry]. At $\epsilon_{CS} = 0.10$, the window is shrunk to zero for $zT = (2.0, 1.0, 0.5)$. In other words, the approximate $SU(2)_{CS}$ symmetry of the z correlators of $\bar{u}\Gamma d$ in $N_f = 2 + 1 + 1$ lattice QCD cannot become a more precise symmetry with $\epsilon_{CS} \leq 0.10$, unlike the $U(1)_A \times SU(2)_L \times SU(2)_R$ chiral symmetry, which is effectively restored as an exact symmetry for $T > T_1 \gtrsim T_c$. Consequently, in the range of temperatures with approximate $SU(2)_{CS}$ symmetry, even if the chromoelectic interactions may play a predominant role in binding u and d quarks into hadron-like objects, the role of chromomagnetic interactions in their bindings cannot be neglected.
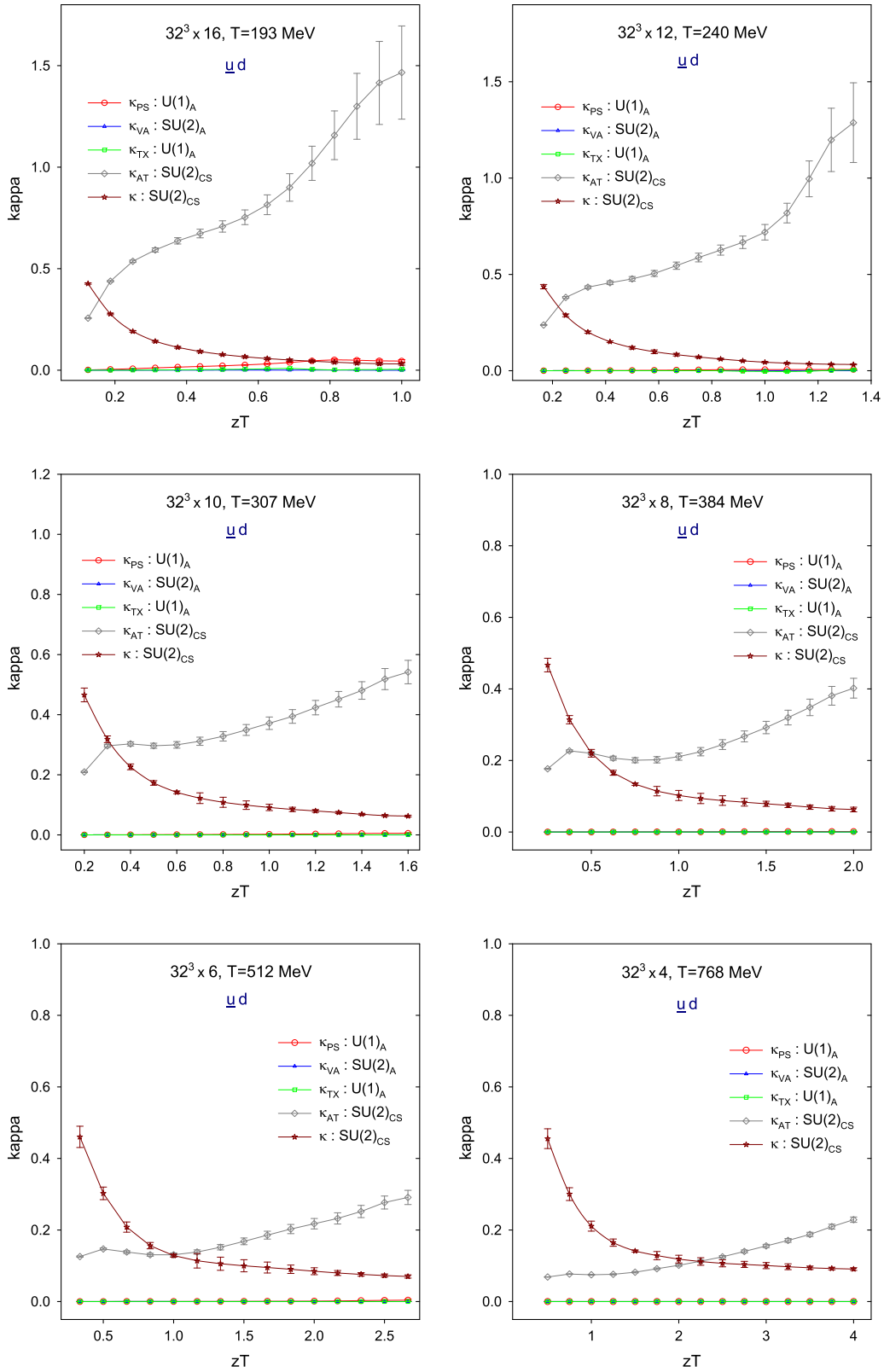
FIG. 8. The symmetry-breaking parameters of z correlators of $\bar{u}\Gamma d$ in $N_f = 2 + 1 + 1$ lattice QCD for six temperatures in the range ~190–770 MeV.
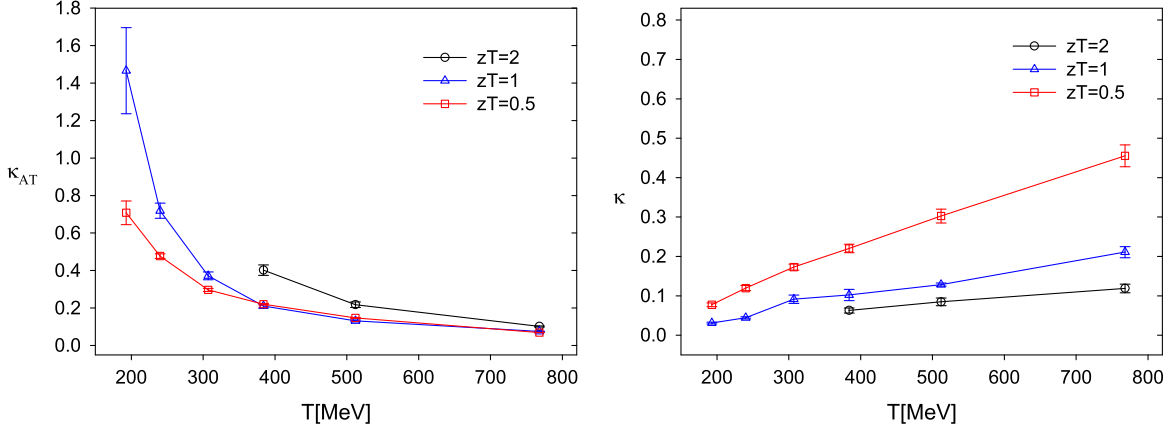
FIG. 9.   The $SU(2)_{\mathrm{CS}}$ symmetry-breaking and -fading parameters ($\kappa_{\mathrm{AT}}, \kappa$) of $N_f = 2 + 1 + 1$ lattice QCD at six temperatures in the range $\sim$190–770 MeV, for $zT = (0.5, 1, 2)$.

C. Comparison with the noninteracting theory

The spatial z correlators of $\bar{u}\Gamma d$ constructed with free-quark propagators are plotted in Fig. 10. The free-quark propagators are computed with the same set of boundary conditions (see Sec. VI A), the same lattice size, and the same u/d quark masses as those in $N_f = 2 + 1 + 1$ lattice QCD, but with all link variables equal to the identity matrix. Note that the lattice spacing a and the temperature $T = 1/(N_t a)$ are not defined for the free quarks. Thus, the label zT of the horizontal axis in Fig. 10 should be regarded as $zT = n_z/N_t$. In the following, the temperature T for all quantities with free quarks is always understood to be the corresponding temperature $T = 1/(N_t a)$ in $N_f = 2 + 1 + 1$ lattice QCD with the same N_t.

In Fig. 10, for all six lattice sizes $32^3 \times (16, 12, 10, 8, 6, 4)$, the $U(1)_A \times SU(2)_L \times SU(2)_R$ chiral symmetry is almost exact in spite of the nonzero u/d quark masses, as shown by the degeneracies $C_P(z) = C_S(z)$, $C_{T_k}(z) = C_{X_k}(z)$, and $C_{V_k}(z) = C_{A_k}(z)$ for $k = 1$, 2, 4. Consequently, it appears that there are only five distinct z correlators in each panel of Fig. 10. They appear in the order

$$C_{T_4,X_4}(\text{free}) > C_{V_1,A_1}(\text{free}) > C_{P,S}(\text{free})$$
$$> C_{V_4,A_4}(\text{free}) > C_{T_1,X_1}(\text{free}), \quad \text{for } n_z \geq 7, \tag{50}$$

which is different from that of $N_f = 2 + 1 + 1$ lattice QCD for $T \sim$ 190–770 MeV in Eq. (47)—i.e.,

$$C_{P,S} > C_{V_1,A_1} > C_{T_4,X_4} > C_{V_4,A_4} > C_{T_1,X_1}, \quad \text{for } n_z \geq 7,$$

where the latter is consistent with that of lattice QCD at $T < T_c \sim 150$ MeV. Note that the orderings of $C_{P,S}$, C_{V_1,A_1}, and C_{T_4,X_4} in Eq. (50) are reversed from those in Eq. (47).

Next, we examine the symmetries in the z correlators of free quarks with the symmetry-breaking parameters as defined in Sec. III.

In Fig. 11, the symmetry-breaking parameters are plotted versus $zT = n_z/N_t$ for $N_t = (16, 12, 10, 8, 6, 4)$. For $U(1)_A$ and $SU(2)_L \times SU(2)_R$ chiral symmetries, $\kappa_{\mathrm{PS}} \simeq \kappa_{\mathrm{TX}} \simeq \kappa_{\mathrm{VA}} < 10^{-7}$, which shows that the $U(1)_A \times SU(2)_L \times SU(2)_R$ chiral symmetry is almost exact in the noninteracting theory with free quarks, in spite of the nonzero u/d quark masses. For the $SU(2)_{\mathrm{CS}}$ symmetry, the symmetry-breaking and -fading parameters $\kappa_{\mathrm{AT}}(zT)$ and $\kappa(zT)$ are much larger than those ($\kappa_{\mathrm{PS}}, \kappa_{\mathrm{TX}}, \kappa_{\mathrm{VA}}$) of $U(1)_A$ and $SU(2)_L \times SU(2)_R$ chiral symmetries.

In Fig. 12, the data of $\kappa_{\mathrm{AT}}(zT)$ and $\kappa(zT)$ in Fig. 11 of the noninteracting theory are plotted versus the corresponding temperature $T = 1/(N_t a)$ in $N_f = 2 + 1 + 1$ lattice QCD with the same N_t, for $zT = n_z/N_t = (0.5, 1, 2)$. In general, for any fixed zT, $|\kappa_{\mathrm{AT}}| \lesssim 0.3$, and $\kappa > 0.89$ for any T. Obviously, there does not exist any window satisfying the criterion of Eq. (41) with $\epsilon_{\mathrm{CS}} < 0.89$. Thus, the $SU(2)_{\mathrm{CS}}$

TABLE IV.   The approximate ranges of temperatures satisfying the criterion in Eq. (41) with $\epsilon_{\mathrm{CS}} = (0.20, 0.15, 0.10)$, for $zT = (2.0, 1.0, 0.5)$. In the second column, T_x (> 770 MeV) and T_y (> 770 MeV) have yet to be determined.

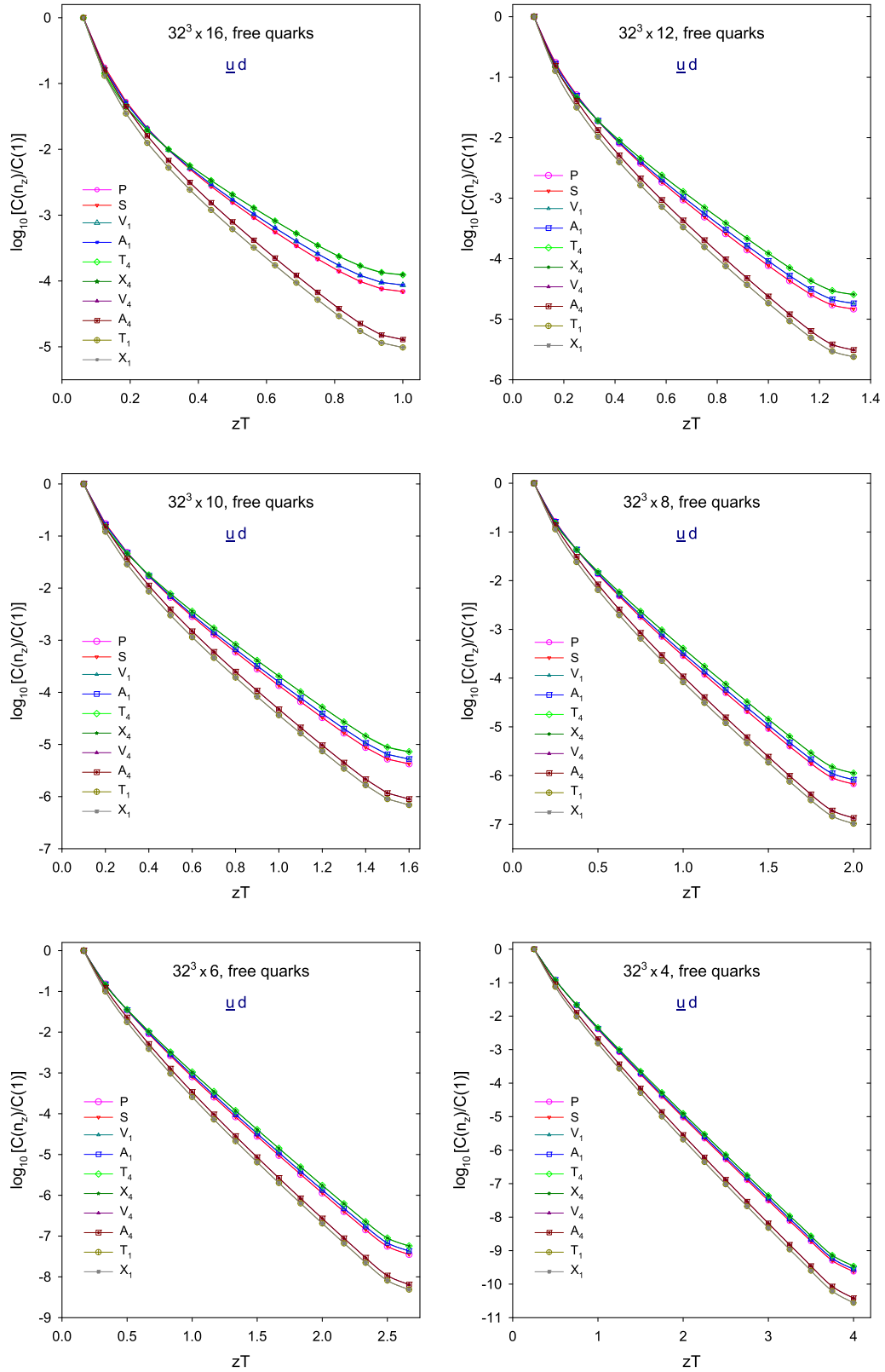| ϵ_{CS}	$zT = 2.0$	$zT = 1.0$	$zT = 0.5$
0.20	$\sim$550 MeV$-T_x$(> 770 MeV)	$\sim$380–730 MeV	NULL
0.15	$\sim$660 MeV$-T_y$(> 770 MeV)	$\sim$480–580 MeV	NULL
0.10	NULL	NULL	NULL

FIG. 10.   The spatial z correlators of $\bar{u}\Gamma d$ meson interpolators constructed with the free-quark propagators.
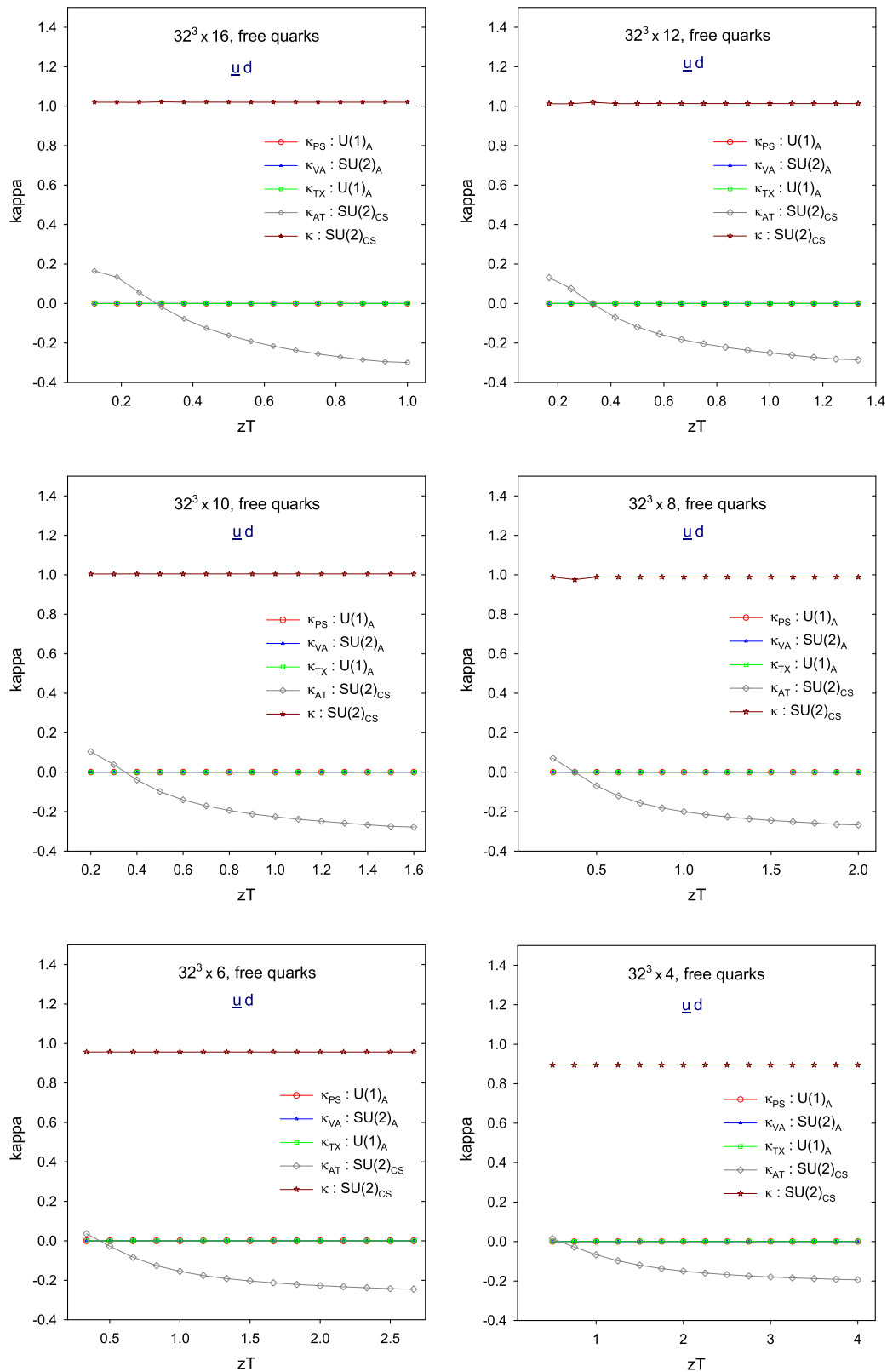
FIG. 11. The symmetry-breaking parameters of the z correlators of $\bar{u}\Gamma d$ with free quarks.
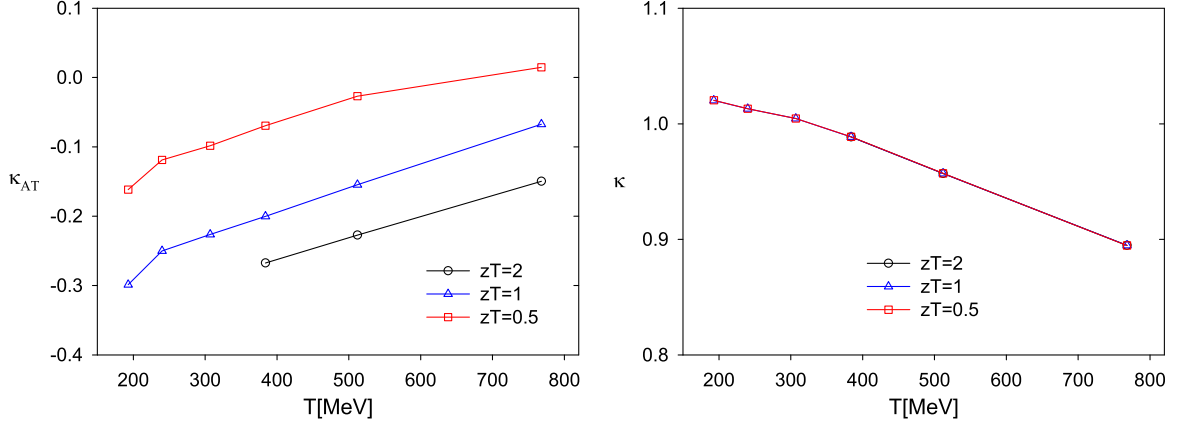
FIG. 12.   The $SU(2)_{CS}$ symmetry-breaking and -fading parameters (κ_{AT}, κ) of the spatial meson correlators with free quarks, versus the corresponding temperature $T = 1/(N_t a)$ in $N_f = 2 + 1 + 1$ lattice QCD with the same N_t, for $zT = n_z/N_t = (0.5, 1, 2)$.

symmetry does not emerge in the noninteracting theory on a lattice, in contrast to the $N_f = 2 + 1 + 1$ lattice QCD at the physical point, with the emergence of approximate $SU(2)_{CS}$ symmetry in the windows, as tabulated in Table IV. This implies that u and d quarks at these temperatures must be dynamically very different from the free or quasifree fermions. If the deconfined quarks in high-temperature QCD behave like free or quasifree quarks, then the u and d quarks in $N_f = 2 + 1 + 1$ lattice QCD at the temperatures with approximate emergent $SU(2)_{CS}$ symmetry are likely to be confined inside hadron-like objects, which are predominantly bound by the chromoelectric interactions into color singlets. Moreover, since $SU(2)_{CS}$ is a rather approximate emergent symmetry, the role of chromomagnetic interactions in forming these hadron-like objects cannot be neglected.

D. Comparison with the $N_f = 2$ lattice QCD

In Ref. [5], the symmetries of z correlators of $\bar{u}\Gamma d$ were studied in $N_f = 2$ lattice QCD with Möbius domain-wall

fermions, using nine ensembles of lattice sizes $[32^3 \times (12, 8, 6, 4)]$ and lattice spacings $[a = (0.051, 0.065, 0.075, 0.096, 0.113)$ fm], covering the temperatures in the range $\sim$220–960 MeV.

Comparing the z correlators of $N_f = 2 + 1 + 1$ lattice QCD in Fig. 7 with those of $N_f = 2$ lattice QCD in Fig. 1 of Ref. [5], we see that in both cases, the order of Eq. (47) is satisfied. Also, the $U_A(1)$ and $SU(2)_L \times SU(2)_R$ chiral symmetries are effectively restored for all studied temperatures, in terms of the degeneracies $C_P(z) = C_S(z)$, $C_{T_k}(z) = C_{X_k}(z)$, and $C_{V_k}(z) = C_{A_k}(z)$ for $k = 1, 2, 4$.

For the $SU(2)_{CS}$ symmetry, its breaking in $N_f = 2 + 1 + 1$ lattice QCD is larger than that in $N_f = 2$ lattice QCD at the same temperature T. This can be seen by comparing the degeneracy in the multiplet $M_2 = (V_1, A_1, T_4, X_4)$ in Fig. 7 with that in Fig. 1 of Ref. [5], and similarly for the multiplet $M_4 = (V_4, A_4, T_1, X_1)$. Moreover, this can be seen by comparing the $SU(2)_{CS}$ symmetry-breaking and -fading parameters $[\kappa_{AT}(zT), \kappa(zT)]$ between $N_f = 2 + 1 + 1$ and $N_f = 2$ lattice QCD.
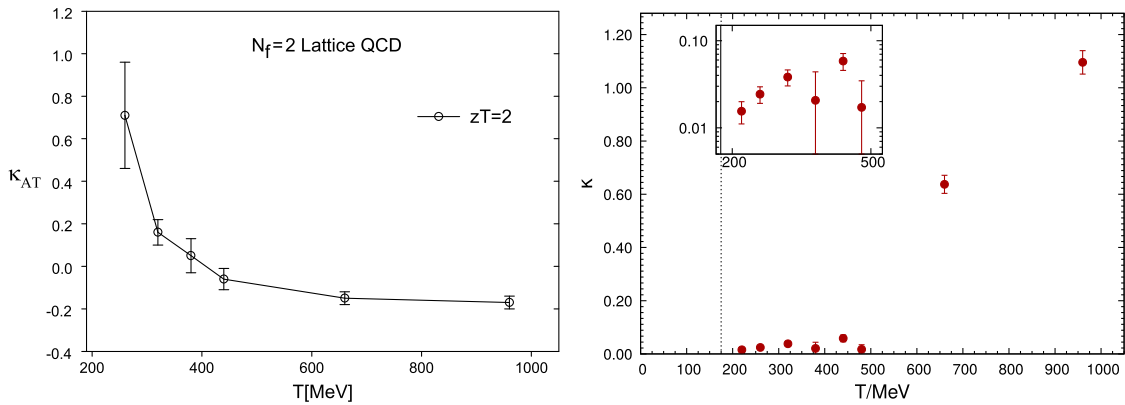

FIG. 13.   The $SU(2)_{CS}$ symmetry-breaking and -fading parameters $(\kappa_{AT}, |\kappa|)$, at $zT = 2$ for six temperatures $T \sim 260$–960 MeV in $N_f = 2$ lattice QCD. The data points of $\kappa_{AT} = C_{A_1}/C_{T_4} - 1$ in the left panel are read off from the ratio C_{A_1}/C_{T_4} shown in Figs. 3 and 4 of Ref. [5], while the right panel exactly matches Fig. 5 of Ref. [5].

TABLE V. The ranges of temperatures satisfying the criterion in Eq. (41) with $\epsilon_{CS} = (0.20, 0.15, 0.10, 0.05, 0.01)$ at $zT = 2.0$, for $N_f = 2$ lattice QCD (Ref. [5]) and $N_f = 2 + 1 + 1$ lattice QCD (this work). The third column ($N_f = 2 + 1 + 1$) is taken from Table IV, where T_x (> 770 MeV) and T_y (> 770 MeV) have yet to be determined.

ϵ_{CS}	$N_f = 2$ [5]	$N_f = 2 + 1 + 1$ (this work)
0.20	~320–500 MeV	~550 MeV$-T_x$(> 770 MeV)
0.15	~326–500 MeV	~660 MeV$-T_y$(> 770 MeV)
0.10	~350–500 MeV	NULL
0.05	~380–430 MeV	NULL
0.01	NULL	NULL

Reading off the ratio $C_{A_1}(zT)/C_{T_4}(zT)$ from Figs. 3 and 4 of Ref. [5], the value of $\kappa_{AT}(zT) = C_{A_1}(zT)/C_{T_4}(zT) - 1$ can be obtained for $N_f = 2$ lattice QCD. At $zT = 2$, the values of κ_{AT} for six temperatures are plotted in the left panel of Fig. 13, while those of $|\kappa|$ are shown in the right panel of Fig. 13, which exactly matches Fig. 5 of Ref. [5].

Using the data of κ_{AT} and κ as shown in Fig. 13 and the criterion in Eq. (41) for the emergence of approximate $SU(2)_{CS}$ symmetry, we obtain the ranges of temperatures satisfying Eq. (41) for $\epsilon_{CS} = (0.20, 0.15, 0.10, 0.05, 0.01)$, as tabulated in the second column of Table V. For comparison, the corresponding results of $N_f = 2 + 1 + 1$ lattice QCD are also tabulated in the third column, which are taken from the second column of Table IV.

First, for a given ϵ_{CS}, the lower bound of the window in $N_f = 2 + 1 + 1$ lattice QCD is shifted to a higher temperature than that in $N_f = 2$ lattice QCD. This is mainly due to the fact that the value of κ_{AT} in the former is larger than that in the latter at the same temperature. Thus, the former needs to go to a higher temperature in order to attain the same value of κ_{AT}.

Second, for $N_f = 2$ lattice QCD, the window satisfying the criterion in Eq. (41) is shrunk as ϵ_{CS} is decreased [i.e., a more precise $SU(2)_{CS}$ symmetry]. On the other hand, for $N_f = 2 + 1 + 1$ lattice QCD, since the upper bounds T_x(> 770 MeV) and T_y(> 770 MeV) have yet to be determined, it is unclear whether the window is shrunk as ϵ_{CS} is decreased from 0.20 to 0.15. Since the window is shrunk to zero as ϵ_{CS} is decreased from 0.15 to 0.10, we speculate that the window is also shrunk as ϵ_{CS} is decreased from 0.20 to 0.15.

Third, the window in $N_f = 2$ lattice QCD is nonzero even when ϵ is decreased to 0.05, while the window in $N_f = 2 + 1 + 1$ lattice QCD has been shrunk to zero for $\epsilon_{CS} \leq 0.10$. Finally, the window in $N_f = 2$ lattice QCD is shrunk to zero as ϵ_{CS} is decreased to 0.01.

Evidently, the $SU(2)_{CS}$ symmetry in $N_f = 2 + 1 + 1$ lattice QCD is a more approximate emergent symmetry than that in $N_f = 2$ lattice QCD.

VII. CONCLUSIONS AND OUTLOOK

In this study, we have generated six gauge ensembles of $N_f = 2 + 1 + 1$ lattice QCD with $(u/d, s, c)$ optimal domain-wall quarks at the physical point, on the $32^3 \times (16, 12, 10, 8, 6, 4)$ lattices with two lattice spacings $a \sim (0.064, 0.069)$ fm, for six temperatures in the range ~ 190–770 MeV, as summarized in Table II. The plan is to complete 17 gauge ensembles with three lattice spacings $a \sim (0.064, 0.069, 0.075)$ fm, which can be used to extract the continuum limit of the observables, for temperatures in the range ~ 160–770 MeV.

Using six gauge ensembles, we computed the temporal and spatial correlators for the complete set of Dirac bilinears (scalar, pseudoscalar, vector, axial vector, tensor vector, and axial-tensor vector), and each for six combinations of quark flavors ($\bar{u}d$, $\bar{u}s$, $\bar{u}c$, $\bar{s}c$, $\bar{s}s$, and $\bar{c}c$). In this paper, we focus on the meson correlators of u and d quarks, while those of other flavor combinations will be analyzed in a forthcoming paper [7].

We examine the implications of these results for the effective restoration of the $SU(2)_L \times SU(2)_R$ and $U(1)_A$ chiral symmetries, as well as the emergence of approximate $SU(2)_{CS}$ chiral spin symmetry in $N_f = 2 + 1 + 1$ lattice QCD, using the symmetry-breaking parameters κ_{PS}, κ_{TX}, κ_{VA}, and (κ_{AT}, κ) as discussed in Sec. III. The window of temperatures for the emergence of approximate $SU(2)_{CS}$ symmetry is determined for temporal and spatial correlators according to the criteria in Eqs. (38) and (41), respectively. Comparing the windows in Table III (of the temporal correlators) with those in Table IV (of the spatial correlators), we see that the former are nonzero for ϵ_{CS} down to 0.05 (at $tT = 0.5$), while the latter are shrunk to zero for $\epsilon_{CS} \leq 0.10$ (at any zT). Theoretically, the temporal and spatial correlators have very different physical contents— e.g., the former are related to the thermal masses of the melting mesons, while the latter are related to the screening masses. Thus, it is not surprising to see that the approximate $SU(2)$ symmetry emerges differently in these two sets of correlators.

Comparing $N_f = 2 + 1 + 1$ lattice QCD (in this work) with $N_f = 2$ lattice QCD in Refs. [5,6], we see that in both cases, the $U_A(1)$ and $SU(2)_L \times SU(2)_R$ chiral symmetries are effectively restored for all studied temperatures, in terms of the degeneracies $C_P(z) = C_S(z)$, $C_{T_k}(z) = C_{X_k}(z)$, and $C_{V_k}(z) = C_{A_k}(z)$, for both spatial and time correlators. However, for the approximate $SU(2)_{CS}$ symmetry, it emerges differently in $N_f = 2 + 1 + 1$ and $N_f = 2$ lattice QCD, as shown in Fig. 4 for the fading parameter κ of the temporal correlators, and by comparing Fig. 9 with Fig. 13 for the $SU(2)_{CS}$ symmetry-breaking and -fading parameters (κ_{AT}, κ) of the spatial correlators. In general, the $SU(2)_{CS}$ symmetry breaking in $N_f = 2 + 1 + 1$ lattice QCD is larger than that in $N_f = 2$ lattice QCD at the same temperature T, for both spatial and temporal correlators.

Comparing the windows for the emergence of approximate $SU(2)_{CS}$ symmetry as tabulated in Table V for $zT = 2.0$, we see that the window of $N_f = 2 + 1 + 1$ lattice QCD is shrunk to zero for $\epsilon_{CS} \leq 0.10$, while that of $N_f = 2$ lattice QCD is nonzero as ϵ_{CS} is decreased to 0.05, and then finally it is shrunk to zero for $\epsilon_{CS} \leq 0.01$.

Since both $N_f = 2$ and $N_f = 2 + 1 + 1$ lattice results have not been extrapolated to the continuum, there are

discrepancies due to the discretization uncertainties. Moreover, even in the continuum limit, there are discrepancies between $N_f = 2 + 1 + 1$ and $N_f = 2$ QCD due to the quantum fluctuations of heavy c and s quarks, which are present in the former but absent in the latter. This can be seen explicitly from the quantum expectation value of the meson correlation function of u and d quarks in $N_f = 2 + 1 + 1$ lattice QCD with exact chiral symmetry,

$$C_\Gamma(t, \vec{x}) = \frac{1}{Z} \int [dU] e^{-A_g(U)} \prod_{f=u,d,s,c} \det\left[(D_c + m_f)(\mathbb{1} + rD_c)^{-1}\right] \text{tr}[\Gamma(D_c + m_u)_{x,0}^{-1} \Gamma(D_c + m_d)_{0,x}^{-1}];$$

$$Z = \int [dU] e^{-A_g(U)} \prod_{f=u,d,s,c} \det\left[(D_c + m_f)(\mathbb{1} + rD_c)^{-1}\right], \tag{51}$$

where $A_g(U)$ is the gauge action at temperature $T = 1/(N_t a)$, D_c is the chirally symmetric Dirac operator [17], and $(D_c + m_f)^{-1}$ is the valence quark propagator [18]. Moreover, the explicit breakings of $U(1)_A$, $SU(2)_L \times SU(2)_R$, and $SU(2)_{CS}$ symmetries due to the quark masses of s and c heavy quarks are much larger than those of u and d light quarks. The former enters Eq. (51) only through the quark determinants, while the latter also enters the meson correlator of each configuration through the u/d quark propagators.

In physical reality, it is necessary to incorporate the b-quark determinant in Eq. (51)—i.e., to perform HMC simulations of $N_f = 2 + 1 + 1 + 1$ lattice QCD with $(u/d, s, c, b)$ quarks [19]. This gives more diverse quantum fluctuations than those in Eq. (51). Moreover, since the b quark is much heavier than (u, d, s, c) quarks, its explicit breakings of $U(1)_A$, $SU(2)_L \times SU(2)_R$, and $SU(2)_{CS}$ symmetries must be much larger than those due to (u, d, s, c) quarks. Consequently, the effective restoration of $U_A(1)$ and $SU(2)_L \times SU(2)_R$ chiral symmetries in $N_f = 2 + 1 + 1 + 1$ lattice QCD would occur at different temperatures from those in $N_f = 2 + 1 + 1$ lattice QCD. Moreover, for the emergence of approximate $SU(2)_{CS}$ symmetry with a fixed ϵ_{CS} in the criteria of Eqs. (41) or (38), the lower bound of the window in $N_f = 2 + 1 + 1 + 1$ lattice QCD is likely to occur at a higher temperature than that in $N_f = 2 + 1 + 1$ lattice QCD. Also, as ϵ_{CS} is decreased, the window of $N_f = 2 + 1 + 1 + 1$ lattice QCD would shrink to zero while the window of $N_f = 2 + 1 + 1$ lattice QCD is still nonzero. The above speculations are based on the scenario of going from $N_f = 2$ to $N_f = 2 + 1 + 1$ lattice QCD, as shown in Table V. Our worry is that the $SU(2)_{CS}$ symmetry might not emerge in lattice QCD with physical (u, d, s, c, b) quarks—say, for $\epsilon_{CS} < 0.5$ in the criteria of Eqs. (41) and (38).

Comparing $N_f = 2 + 1 + 1$ lattice QCD at the physical point with the noninteracting theory on the lattice, we see

that u and d quarks behave dynamically very differently from the free (and quasifree) fermions, since the $SU(2)_{CS}$ symmetry does not emerge in the latter, in contrast to the former with the approximate emergent $SU(2)_{CS}$ symmetry in the windows as tabulated in Tables III and IV. If the deconfined quarks in high-temperature QCD behave like free or quasifree fermions, then the u and d quarks in $N_f = 2 + 1 + 1$ lattice QCD at the temperatures with approximate emergent $SU(2)_{CS}$ symmetry are likely to be confined inside hadron-like objects, which are predominantly bound by the chromoelectric interactions into color singlets. Nevertheless, the role of chromomagnetic interactions in forming these hadron-like objects cannot be neglected, since the emergent $SU(2)_{CS}$ symmetry is not an exact symmetry. It is interesting to find out the relationship between the degree of dominance of the chromoelectric interactions in these hadron-like objects and the ϵ_{CS} in the criteria of Eqs. (38) and (41).

To clarify the nature of these meson-like objects, it is necessary to examine the spectral functions of the $J = 1$ mesons (i.e., V_k, A_k, T_k, and X_k) which are relevant to the $SU(2)_{CS}$ symmetry. If bound-state peaks exist in the spectral functions of the $J = 1$ mesons, in the window (T_{CS}, T_f) of the emergence of approximate $SU(2)_{CS}$ symmetry, and also the widths of these peaks gradually broaden, and the peaks eventually disappear as $T \to T_f$, similar to what has been observed in the spectral function of the $J = 0$ mesons (P, S) for $N_f = 2$ lattice QCD [20], then the degrees of freedom in the $J = 1$ mesons can be asserted to be color-singlet (melting) mesons rather than deconfined quarks and gluons. To this end, it is necessary to generalize the approach of Refs. [21,22] for $J = 0$ mesons to $J = 1$ mesons. Also, the spatial correlators of $J = 1$ mesons are required to be evaluated to high precision even at large distances, without the contamination of unphysical meson states, such that the damping factor $D_{m,\beta}(\vec{u})$ [22] of each $J = 1$ meson channel can be extracted reliably.

The proposed prescription in Sec. VI A provides a viable way to attain this goal—that is, to compute two sets of quark propagators with periodic and antiperiodic boundary conditions in the z direction, while their boundary conditions in (x, y, t) directions are the same [i.e., periodic in the (x, y) directions, and antiperiodic in the t direction]. Then, each set of quark propagators is used to construct the z correlators independently, finally taking the average of these two spatial z correlators. Finally, there is another viable prescription for eliminating the contribution of the unphysical meson states, as follows: First, the backward $(-\hat{z})$ running quark propagator is eliminated for each configuration by averaging two quark propagators with periodic and antiperiodic boundary conditions in the z direction. Then, the resulting quark propagator is used for constructing the z correlators of this configuration. Consequently, the z correlators are free of backward-propagating meson states as well as the unphysical meson states, and they behave like $\sim e^{-Mz}$ rather than $\sim \cosh[M(L_z/2 - z)]$. The advantage of the new

prescription is that the effective mass $M_\Gamma^{\text{eff}}(z) = \ln[C_\Gamma(n_z)/C_\Gamma(n_z + 1)]$ has a longer plateau than that of the proposed prescription in Sec. VI A, which is essential for the determination of screening mass reliably. Once two sets of quark propagators with periodic and antiperiodic boundary conditions in the z direction are computed, then the z correlators of these two prescriptions can be constructed respectively.

[1] C. E. DeTar and J. B. Kogut, The Hadronic Spectrum of the Quark Plasma, Phys. Rev. Lett. **59**, 399 (1987); Measuring the Hadronic Spectrum of the Quark Plasma, Phys. Rev. D **36**, 2828 (1987).

[2] A. Bazavov, S. Dentinger, H. T. Ding, P. Hegde, O. Kaczmarek, F. Karsch, E. Laermann, A. Lahiri, S. Mukherjee, H. Ohno *et al.*, Meson screening masses in (2 + 1)-flavor QCD, Phys. Rev. D **100**, 094510 (2019).

[3] L. Y. Glozman, $SU(4)$ symmetry of the dynamical QCD string and genesis of hadron spectra, Eur. Phys. J. A **51**, 27 (2015).

[4] L. Y. Glozman and M. Pak, Exploring a new $SU(4)$ symmetry of meson interpolators, Phys. Rev. D **92**, 016001 (2015).

[5] C. Rohrhofer, Y. Aoki, G. Cossu, H. Fukaya, C. Gattringer, L. Y. Glozman, S. Hashimoto, C. B. Lang, and S. Prelovsek, Symmetries of spatial meson correlators in high temperature QCD, Phys. Rev. D **100**, 014502 (2019).

[6] C. Rohrhofer, Y. Aoki, L. Y. Glozman, and S. Hashimoto, Chiral-spin symmetry of the meson spectral function above T_c, Phys. Lett. B **802**, 135245 (2020).

[7] T. W. Chiu (to be published).

[8] T. W. Chiu, Optimal Domain Wall Fermions, Phys. Rev. Lett. **90**, 071601 (2003); Domain-wall fermion with R_5 symmetry, Phys. Lett. B **744**, 95 (2015).

[9] T. W. Chiu, T. H. Hsieh, and Y. Y. Mao (TWQCD Collaboration), Pseudoscalar meson in two flavors QCD with the optimal domain-wall fermion, Phys. Lett. B **717**, 420 (2012).

[10] Y. C. Chen and T. W. Chiu (TWQCD Collaboration), Exact pseudofermion action for Monte Carlo simulation of domain-wall fermion, Phys. Lett. B **738**, 55 (2014).

[11] Y. C. Chen, T. W. Chiu, and T. H. Hsieh (TWQCD Collaboration), Topological susceptibility in finite temperature QCD with physical (u/d, s, c) domain-wall quarks, Phys. Rev. D **106**, 074501 (2022).

[12] R. Narayanan and H. Neuberger, Infinite N phase transitions in continuum Wilson loop operators, J. High Energy Phys. 03 (2006) 064.

[13] M. Luscher, Properties and uses of the Wilson flow in lattice QCD, J. High Energy Phys. 08 (2010) 071; 03 (2014) 92.

[14] A. Bazavov *et al.* (MILC Collaboration), Gradient flow and scale setting on MILC HISQ ensembles, Phys. Rev. D **93**, 094510 (2016).

[15] Y. C. Chen and T. W. Chiu (TWQCD Collaboration), Chiral symmetry and the residual mass in lattice QCD with the optimal domain-wall fermion, Phys. Rev. D **86**, 094508 (2012).

[16] L. Y. Glozman and C. B. Lang, A finite box as a tool to distinguish free quarks from confinement at high temperatures, Eur. Phys. J. A **57**, 182 (2021).

[17] T. W. Chiu and S. V. Zenkin, On solutions of the Ginsparg-Wilson relation, Phys. Rev. D **59**, 074501 (1999).

[18] T. W. Chiu, GW fermion propagators and chiral condensate, Phys. Rev. D **60**, 034503 (1999).

[19] T. W. Chiu, Beauty mesons in $N_f = 2 + 1 + 1$ lattice QCD with exact chiral symmetry, Phys. Rev. D **102**, 034510 (2020).

[20] P. Lowdon and O. Philipsen, Pion spectral properties above the chiral crossover of QCD, J. High Energy Phys. 10 (2022) 161.

[21] J. Bros and D. Buchholz, Particles and propagators in relativistic thermo field theory, Z. Phys. C **55**, 509 (1992).

[22] J. Bros and D. Buchholz, Asymptotic dynamics of thermal quantum fields, Nucl. Phys. **B627**, 289 (2002).